Resilience-Constrained Expansion Planning of Integrated Power-Gas-Heat Distribution Networks

Sabzpoosh Saravi, Seyed Vahid; Kalantar, Mohsen; Anvari-Moghaddam, Amjad

Published in:
Applied Energy

DOI (link to publication from Publisher):
10.1016/j.apenergy.2022.119315

Publication date:
2022

Document Version
Accepted author manuscript, peer reviewed version

Highlights

Resilience-Constrained Expansion Planning of Integrated Power-Gas-Heat Distribution Networks

Seyed Vahid Sabzpoosh Saravi,Mohsen Kalantar,Amjad Anvari-Moghaddam

- A stochastic expansion planning model is proposed for integrated energy networks
- An efficient and privacy-preserving approach is used to solve the optimization model
- A resilience index is proposed to evaluate suitability of solutions in long-term planning
- A framework for the interaction among integrated distribution networks is proposed

Resilience-Constrained Expansion Planning of Integrated Power-Gas-Heat Distribution Networks

Seyed Vahid Sabzpoosh Saravi[a], Mohsen Kalantar[a,*] and Amjad Anvari-Moghaddam[b]

[a]Department of Electrical Engineering, Iran University of Science and Technology, Tehran, Iran
[b]Department of Energy (AAU Energy), Aalborg University, 9220 Aalborg, Denmark

ARTICLE INFO

Keywords:
Integrated distribution networks
Stochastic expansion planning
Resilience index
Linearized alternating methods of multipliers
Hurricane

ABSTRACT

Integrated energy systems (IESs) have attracted wide attention as effective frameworks to develop efficient use of energy resources. Proactive preparedness is a sensible approach for integrated distribution networks (IDNs) to propitiously cope with high-impact rare (HR) events. In this paper, a resilient-constrained two-stage expansion planning methodology is proposed with the aim of simultaneously optimal expansion of the IDNs and resilience improvement against hurricanes in long-term. To maintain the independence of IDN's operation and to cope with the computational complexity of such large-scale planning problem, a modified linearized alternating direction method of multipliers with parallel splitting and the adaptive penalty (LADMMPSAP) is introduced to convert the centralized model to a decentralized one. Accordingly, a new framework for the interaction between IDNs is proposed with the resilience and energy coordinator unit (RECU), which is responsible for couplings coordination between IDNs. The main goal of stage 1 is to minimize total cost, which includes investment, operation, and resilience costs. The optimal expansion scheme with optimal operation strategies is obtained in this stage. A stochastic resilience maximization under hurricane occurrence scenarios is modeled in stage 2. A normalized resilience index (RI) for evaluating resilience in IDNs suitable for long-term planning is proposed. The priorities of lines hardening and tie-line installation are determined using the proposed resilience importance index (RII) in stage 2 and sent back to stage 1. The effectiveness of the proposed methodology is tested on real-scale IDNs. The simulation results depict the privileges of incorporating resilience in long-term expansion planning from both economic and technical aspects.

1. Introduction

Nowadays, energy system planning and operation are done separately by types of energy sectors (e.g., electricity, gas, heat). In contrast, an integrated energy system (IES) connects different energy sectors with the objections of energy efficiency, cost-effective investment, increasing renewable energy utilization, and reliability of IESs. The result is increased energy efficiency and tackling environmental pollution, which is among the present significant concerns in the world. With the increased penetration of power-to-gas (P2G) and gas-to-power (G2P) technologies, especially combined heat and power(CHP) units, coordinated expansion planning of electricity, gas, and heat distribution networks becomes a challenging task. IESs can incorporate renewable energy resources effectively through advanced energy conversion technology, which are more economical and environmentally friendly and thus combat climate change [1]. The high penetration of multi-energy technologies like CHPs, gas boilers (GBs), electric boilers (EBs), and heat pumps (HPs) and ongoing transformation in energy sectors present increasingly strong interactions among information, electricity, gas, heat, and transport networks [2]-[3]. Accordingly, energy system planning is affected by such growing interactions between different kinds of energy networks. The planning decision is influenced by the preference of energy utilization, geographical location, and situation of energy distribution [4]. New challenges are posed for traditional planning strategies specially in handling the interactions between energy sectors. Therefore, a combined co-planning approach is highly needed to expand integrated distribution networks (IDNs) economically and environmentally friendly. Contrary to power distribution networks (PDNs) planning, the literature on natural gas distribution (GDNs) planning is much limited. Integrated coordination of power and gas networks should be considered from operational and long-term planning aspects [5].

In recent years, some research has been conducted to solve expansion planning optimization problems in IDNs, mainly combining two types of distribution networks such as power-gas or power-heat. Integrating natural gas and electricity sectors requires examining their interactions and resource co-optimization, usually from a central planner perspective [6]. A co-planning model for integrated power and natural gas systems to minimize total investment and operation costs is presented in [7]. A joint N-1 and probabilistic reliability criterion is included in the model using two sub-problems. The authors conclude that the defined criterion can guarantee the overall system reliability. An expansion planning problem considering the interconnection of natural gas and electricity energy infrastructures is addressed in [8]. The main goal of the proposed model is to optimally select network elements, and expand electric power lines and natural gas pipelines, in order to achieve a satisfying reliability performance. Some research has been developed stochastic models for IESs expansion planning. In [9] a stochastic expansion planning of gas and power networks is carried out in which wind power and load growth uncertainties are considered.Multi-stage stochastic programming model is investigated in [10] to study the sequential investment

*Corresponding author
vahid_Sabzpoosh@elec.iust.ac.ir (S.V.S. Saravi); kalantar@iust.ac.ir (M. Kalantar); aam@energy.aau.dk (A. Anvari-Moghaddam)
ORCID(s):

Nomenclature

Indices

T, T^g, T^s, T^L	Indices of planning period, generation, storage and, line useful lifetime
$y, \mathbb{s}, t$	Indices of years, seasons, and time
g, s, L	Indices of generation, storage units and lines
i, j	Indices of PDN buses
k, l	Indices of GDN nodes
m, r	Indices of DHN nodes
$\hat{ik}, \hat{im}, \hat{km}, \hat{ki}$	Indices of connected buses/nodes between IDN's
$slack$	Index of slack bus/node
N	Index of networks E,G,H
ν	Index of wind speed profile
c	Index of spatial coordinates
Pu, Co	Indices of pumps and compressors

Sets

$\Omega_{\mathbb{s}}$	Set of seasons
T_d	Set of daily load periods in seasons
T_e	Set of emergency load periods in years
Ω_N	Set of distribution networks
$\Omega^{(n)}_{N,g}$	Set of new generation units
$\Omega^{(n)}_{N,s}$	Set of new storage units
$\Omega^{(n,e)}_{N,L}$	Set of new and existing lines
Ω_{TL}	Set of candidate tie-lines in the PDN
Ω_f	Set of buses/nodes with demand curtailment
$\Omega^f_{E,L}$	Set of damaged lines in the PDN
$\Omega_{E,n}, \Omega_{G,n}, \Omega_{H,n}$	Sets of buses/nodes in the PDN, GDN and DHN
$\Omega_{E,g}, \Omega_{G,g}, \Omega_{H,g}$	Sets of generation units in the PDN, GDN and DHN
$\Omega_{E,s}, \Omega_{G,s}, \Omega_{H,s}$	Sets of storage units in the PDN, GDN and DHN
$\Omega_{CHP}, \Omega_{P2G}$	Sets of CHP and P2G units
Ω_{EB}, Ω_{GB}	Sets of electric and gas boilers
$\Omega_{Co}, \Omega_{L,Co}, \Omega_{Pu}$	Sets of compressors, lines with compressor and pumps
$\Omega^{CHP}_{E,n}, \Omega^{P2G}_{E,n}$	Sets of PDN buses with CHP and P2G
$\Omega^{EB}_{H,n}, \Omega^{GB}_{H,n}$	Sets of DHN nodes with EB and GB

Parameters

Pr_ζ	Probability of scenario ζ
IR_ζ	Interest rate in scenario ζ
$N_{\mathbb{s}}$	Number of days in season $\mathbb{s}$
N_H	Number of hurricanes in a year
$\rho^H_{\mathbb{s}}$	Probability of hurricane occurrence in each season
$R_{N,g}, R_{N,s}$	Rated capacity of generation and storage units
$C^I_{N,g}, C^I_{N,s}, C^I_{N,L}$	Investment costs (per unit) of generation and storage units, and lines
$C^O_{N,g}, C^O_{N,s}, C^O_{N,L}$	Annual operation costs of generation units, storage units and lines
$L^{(n)}_{E,ij}, L^{(r)}_{E,ij}$	Lengths of new and reinforced lines
$C^{(r)}_{E,L}$	Reinforcement cost of lines in the PDN
$C^{EC}_{N,g,y,\mathbb{s},t}$	The energy carrier prices in the IDNs
$C^{retail}_{N,y,\mathbb{s},t}$	Retail price of energy in the IDNs
$C^{LD}_{N,y,\mathbb{s},t}$	Lost demand unit value in the IDNs
Δt	Duration of each time period
C^{repair}_p	Repair cost of failed power poles
C^{FP}	Number of failed power poles
C_{Budget}	Annual budget
G_{ii}, G_{ij}	Self and mutual conductance of power lines
B_{ii}, B_{ij}	Self and mutual susceptance of power lines
Z^L_{ij}	Impedance of power lines
$\psi_{G,kl}, \psi_{H,mr}$	Weymouth constant for gas and heat pipelines
$\overline{S}^{Imp}_{E,t}$	Maximum imported apparent power from upstream power grid
$\overline{P}^{loss}_{E,ij}$	Upper limit for active power loss of line ij
$\overline{P}_{E,s}, \overline{q}_{G,s}, \overline{M}_{H,s}$	Capacity of electric, gas, and thermal storage units
$P^D_{E,i,t}, Q^D_{E,i,t}$	Active and reactive power demands
$P^{D,Ncr}_{E,i,t}$	Non-critical active power demands
$q^D_{G,k,t}, m^D_{H,m,t}$	Gas and heat demands
$q^{D,Ncr}_{G,k,t}, m^{D,Ncr}_{H,m,t}$	Non-critical gas and heat demands
ξ_{kl}	Compression coefficient in active gas pipelines
k_1, k_2	A constant and isentropic coefficient of natural gas
$\underline{C}R, \overline{C}R$	Lower and upper limits of compressor compression ratio
$\eta^{ch}_{N,s}, \eta^{dis}_{N,s}$	Conversion efficiencies of storage units in related network N
φ_{mr}	Heat loss coefficient of heat pipelines
$\eta^{CHP,e}_{i,g}, \eta^{CHP,hl}_{i,g}$	Generating and heat loss of CHP units
$\beta^{CHP}_{i,g}$	Heat exchange coefficients of CHP units
$\eta^{P2G}_{i,g}, \eta^{EB}_{m,g}, \eta^{GB}_{m,g}$	Energy conversion coefficient in P2G, EB, and GB
P^f_{Th}	Failure probability thresholds
$P^f_{Po_u}, P^f_{Co_w}$	The failure probability of pole u and conductor w
ω_N	The importance weight of network N
μ, λ	Adaptive penalty parameter, penalty factor
ρ, σ	Adaptively updated parameter and a constant

Variables

$x_{N,g,y}, x_{N,s,y}$	Binary investment variables for generation and storage units
$x_{N,L,y}, x^r_{E,L,y}$	Binary investment and reinforcement variables for lines

$x^{ch}_{N,s,t}$	Statuses of storage units; charging (1), discharging (0)	$\Gamma_{G,k,t}$	Gas pressure at node k at time t
$E_{N,g,y,\mathbb{s},t}$	Energy produced by generator g in year y, season $\mathbb{s}$ at time t	$m_{H,m,g,t}$, $M_{H,m,g,t}$	Water mass flow and heat supply of source g at node m at time t
$D^{NS}_{N,i/k/m,y,\mathbb{s},t}$	The demand not supplied at bus/node $i/k/m$ in year y, season $\mathbb{s}$ and time t	$M^{curt}_{H,m,t}$	Heat demand curtailment at node m at time t
$P_{E,i,g,t}, Q_{E,i,g,t}$	Active and reactive power of generator g at bus i at time t	$M^{ch}_{H,m,s,t}, M^{dis}_{H,m,s,t}$	Charging and discharging heat of thermal storage s at node m at time t
$P^{curt}_{E,i,g,t}, Q^{curt}_{E,i,g,t}$	Active and reactive power demand curtailment at bus i at time t	$m_{H,mr,t}$	Water flow through pipeline mr at time t
$P^{ch}_{E,i,s,t}, Q^{dis}_{E,i,s,t}$	Charging and discharging power of storage s at time t	$\Pi_{H,m,t}$	Water pressure of node m at time t
$P_{E,ij,t}, Q_{E,ij,t}$	Active and reactive power flow in line ij at time t	$\tau^{in}_{H,mr,t}, \tau^{out}_{H,mr,t}$	Inlet and outlet temperature of pipeline mr at time t
$V_{i,t}, \theta_{i,t}$	Voltage magnitude and angle of bus i at time t	$\tau^{mix}_{m,t}$	Mixed temperature of node m at time t
$P^{Imp}_{E,t}, Q^{Imp}_{E,t}$	Imported power to upstream grid at time t	τ^{a}	Ambient temperature
$SoC_{N,s,t}$	State of charge in storage s at time t	$P^{D,P2G}_{E,i,t}, P^{D,EB}_{E,m,t}$	Power consumption of P2G and EB at bus i and node m at time t
$q_{G,k,g,t}$	Gas flow of source g at node k at time t	$P^{D,GC}_{G,k,t}, P^{D,WP}_{H,m,t}$	Power consumption of GC, and WP at node k and m at time t
$q^{curt}_{G,k,t}$	Gas demand curtailment at node k at time t	$q^{D,GB}_{E,m,t}, q^{D,CHP}_{G,i,t}$	Gas consumption of GB and CHP at node m and bus i at time t
$q^{ch}_{G,k,s,t}, q^{dis}_{G,k,s,t}$	Charging and discharging flows of gas storage s at node k at time t	$D_{N,t}, D^{nor}_{N,t}$	Supplied demand and normalized demand of network N at time t
$q_{G,k,t}, q_{G,c,t}, q_{G,kl,t}$	Gas flow in node k, compressor c and pipeline kl at time t	δ	Lagrangian multiplier

decision with the uncertainties revealed gradually over time, where constraints in power and gas systems are considered.

The role of energy storage facilities in IESs has been investigated in some studies. A long-term planning study using a two-stage chance-constrained model for integrated gas and power systems is presented in [11] highlighting the role of natural gas storage in mitigating the effect of uncertainties in operation. Since P2G could be a good option for long-term storage in IES, integrated expansion planning of gas and power networks considering P2G units and gas-fired devices is investigated in [12–14]. A comprehensive stochastic IES planning framework that accommodates the cap-and-trade market and P2G investment options is presented in [14]. The effects of incorporating multi-carrier energy storage technologies on the optimal scheduling of integrated power, gas, and heat networks are addressed in [15]. In [16], the authors propose an integrated demand response model which coordinates flexible loads, P2Gs, HPs, and energy storage systems (ESSs).

Quite a few studies have been conducted to address the expansion planning of IESs considering the interdependency issues and the economic and resilient operation of IESs [17]. A total cost minimization objective function is developed, focusing on the optimal determination of the infrastructure's technologies, size, and location. A multi-temporal simulation model for analyzing IDNs including PDN, GDN, and DHN is proposed in [18]. The coupling of networks has been modeled using a multi-vector efficiency matrix, and the integrated networks flow has been solved simultaneously through the Newton-Raphson method. The energy hub concept has been investigated in some studies for modeling of IESs expansion planning models. An expansion planning model for multi-energy system integrating active PDN, GDN, and energy hub is developed in [19], which explore the influence of active PDN management on multi-energy system expansion. An optimal operation strategy for the multi-carrier energy system within the energy hub framework model is conducted. An optimal expansion planning within energy hub coupling electricity, natural gas, and heat energy system is proposed in [20] where the plans are evaluated with reliability, energy efficiency, and emission matrices. A two-stage mixed-integer linear programming (MILP) approach for optimal planning of IESs is proposed in [21]. The first stage is optimizing the selection of candidate elements in a three-layered energy hub, and the second stage is optimizing the connection path for the selected elements of the first stage in every two adjacent layers.

The concept of network resilience against high-impact rare (HR) events has received wide attention recently since natural disasters can cause severe and wide-spreading effects, including shortage of power, gas, and district heating supplies for large parts of the distribution network demands [22]. Hurricane Sandy, for example, caused the inaccessibility of about 7 million people to electric power in North America and many water pumps (WPs) outages, and loss of clean water in New York City in 2012 [23]. 90% of faults due to natural disasters occurs in PDNs [24]. According to the findings of [25], if the world becomes 3 to 4 degrees

warmer due to greenhouse gas emissions in this century, the frequency of hurricanes will increase by 30%; concurrently, the wind speed can be intensified up to 13 m/s. Therefore, the resilience of distribution networks is of particular importance and should be studied in the expansion planning of distribution network's long-term programs.

DG integration, network reconfiguration, and network reinforcement provide alternatives approaches to make a PDN more flexible and resilient. Authors of [26] proposed a reliability-constrained expansion planning model for PDN using a MILP model. The model incorporates a defined reliability index in the proposed multi-stage PDN expansion planning problem. Therefore, the planner can achieve an optimal plan simultaneously accounting for investment, operation, and reliability. In [2], a tri-level optimization-based decision support tool is proposed to enhance the resilience of a coupled PDN-urban transportation system in HR events. A two-level planning model for integrated power and gas networks considering a resilient scheduling strategy is studied in [27] to improve the adaptation to the resilience requirements in actual operation. A two-level planning approach for integrated electricity and gas energy systems is proposed in [28] that considers a short-term resilience scheduling strategy to determine the optimal configuration along with the operation. A stochastic model with a central problem and two sub-problem is proposed in [24] to improve the resilience of integrated power and water distribution networks. The main problem is to minimize power and water load outages against hurricanes and investment cost of strategies. In the above mentioned researches, resilience improvement has been studied in the form of a short-term planning problem.

The data exchange infrastructure among different energy systems in IESs is rarely investigated in the previous literature. Centralized expansion planning of IDNs implicitly assumes a vertically integrated structure while these distribution networks are independent energy parties. So a practical approach is required to address the proposed resilience-constrained expansion planning problem as a tripartite problem. The alternating direction method of multipliers (ADMM) can convert the proposed centralized problem to a decentralized one. The ADMM can be used for only two blocks of variables. A central coordinator using the ADMM for integrated gas and electricity networks is introduced in [9], which preserves the privacy of gas and electricity networks. Decentralized problems based on ADMM have been studied in recent years, such as utilizing distributed scheduling frameworks to distinguish different energy parties as independent stakeholders [29]-[30]. For a problem with more than two blocks of variables and a complex objective function, ADMM may not converge [31]. Linearized ADMM with Parallel Splitting and Adaptive Penalty (LADMMPSAP) is proposed in [32] which fits for more than two blocks of variables and helps to faster convergence. The LADMMPSAP method introduced in this paper is inherited from [32], except that some modification has been made in variable updating and stop criteria.

Unlike numerous works which have been studied the expansion planning of individual PDNs against hurricanes in recent years, a few works have investigated the expansion planning of integrated PDN, GDN and DHN. To the best of the author's knowledge, the following aspects are still research gaps:

(1) The comprehensive IDNs (including PDN, GDN, and DHN) expansion planning considering the interaction between distribution networks under HR events has not been reported in the literature.
(2) The reality-based decentralized structure of IDNs in a multi-energy system with high dependency levels has not been comprehensively investigated. The role of the coordinator unit in the decentralized model considering HR events needs research.
(3) Some research has been done for resilience improvement in short-term planning, but comprehensive long-term expansion planning incorporates resilience planning, has not been reported in the literature.

To fill the mentioned gaps, the resilience-constrained two-stage integrated distribution networks stochastic expansion planning (IDNSEP) model is originally proposed. The IDNs are composed of PDN, GDN, and DHN. In stage 1, a comprehensive expansion planning model with total cost minimization objective is proposed, which focuses on the optimal determination of technology, location, and size of candidate generation units, storage units, and distribution lines in IDNs. The resilience maximization under hurricane occurrence scenarios is modeled in stage 2. The optimal reinforcement and tie-line installation strategies are determined in stage 2. The optimal tie-line installation helps to obtain optimal reconfiguration in operation mode. To make the planning model robust and more accurate, the stochastic framework is adopted in both stages. The key contributions of this paper can be summarized as follows:

(1) A stochastic two-stage expansion planning model for IDNs is proposed, which considers resilience in long-term planning.
(2) A new framework for the interaction between IDNs is proposed where the resilience and energy coordinator unit (RECU) is responsible for couplings coordination between IDNs.
(3) LADMMPSAP is introduced to convert the centralized model to a decentralized one; using this, the proposed complex model can be efficiently solved.
(4) A normalized resilience index (RI) for evaluating resilience in IDNs is proposed, which considers both disruption and recovery phases and is proper for evaluating resilience in long-term planning. Also, using this RI, a resilience importance index (RII) is proposed, which determines the priorities of lines hardening value and tie-line installation in improving resilience of the IDNs under hurricane occurrence.

The remainder of this paper is organized as follows: Section 2 explains the interactive framework of the proposed two-stage IDNSEP and modelling of each stage. In Section 3 the

solution methodology is described and the flowchart of the proposed methodology is presented. Section 4 elaborates on the simulation results and numerical analysis of case studies. Finally, Section 5 concludes the paper.

2. Proposed two-stage IDNSEP interactive framework

Fig. 1 shows the main problem, objective and output of each stage and also the relation between the two stages of the proposed IDNSEP method. Stage 1 runs both in normal and emergency periods of the study while stage 2 runs only in the emergency period. To make the synergy happen among different vectors, different types of information such as power, gas, and heat consumption of networks have to be exchange among integrated networks. In the proposed framework in this paper, the central expansion planning model is converted to a decentralized model using the LADMMPSAP not only to facilitate the synergy, but also to preserve the privacy of IDNs, which decomposes the central optimization problem into three local optimization sub-problems. Each of the distribution networks only exchanges information about coupling variables between IDN's with the coordinator agent (not with other system's operators) while developing the expansion plans on its own thus the privacy of each sector will be preserved in an environment with different uncertainties. In a centralized model, the problem should however be solved by a single agent with the information from all parties which in turn reduces the independence of distribution system operators in decision-making act and the privacy of critical information within each sector (which might be exposed to unauthorized access). Therefore, the expansion planning problem will be solved locally for each distribution network, and the coupling constraints will be checked by the coordinator unit. The repetitive process of exchanging data between distribution networks and the coordinator unit continues until the agreements at the coupling points are reached. The framework of the examined IDNs is shown in Fig. 2. In this section, the proposed two-stage IDNSEP, including the objective function and operation constraints of the PDN, GDN, and DHN are mathematically formulated. The optimization problem formulation at stage 1 is expressed in Section 2.1 with detailed operation constraints in the IDNs. Problem formulation of Stage 2 which includes island formation, reconfiguration, candidate tie-line installation, and PDN's reinforcement prioritizing using the proposed RII, is presented in Section 2.2. Then, in Section 2.3, using the LADMMPSAP, the central expansion planning model is decomposed into three sub-problems which are coupled through the proposed RECU. The LADMMPSAP algorithm is used to solve the linearized model to obtain a convergent solution.

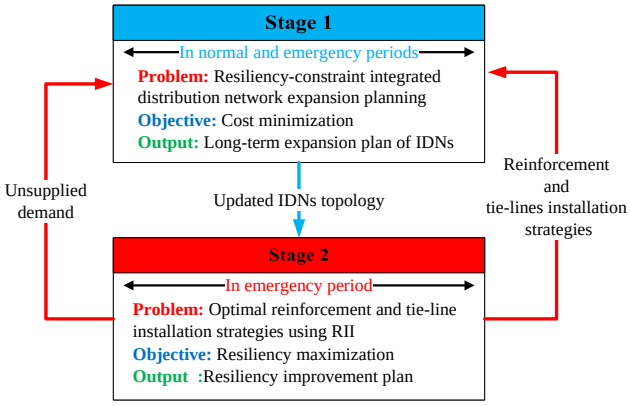

Figure 1: The proposed two-stage IDNSEP structure

2.1. Formulation of stage 1 objective function

An analytical expression for the reliability-constraint formulation of multi-stage PDN planning is proposed in [26], which jointly accounts for economic and reliability. In this paper, a resilience-constrained formulation for IDNs expansion planning is developed based on the general mathematical model in [26]. Also, IDNs are considered to determine the effects of co-planning and the resilience of IDNs in long-term expansion. The proposed model can be cast in a simple representation form as follows:

$$\underset{x,y,z}{Min}\ C^{I,PV}(x,y) + C^{O,PV}(x,y) + C^{RI,PV}(z) \tag{1}$$

$$x \in \{0,1\}^n \tag{2}$$

$$f(x,y) <= 0 \tag{3}$$

$$g(x,z) <= 0 \tag{4}$$

where $C^{I,PV}(x,y)$, $C^{O,PV}(x,y)$, and $C^{RI,PV}(z)$ are the present values of investment, operational and resilience costs, respectively. The resilience cost function represents the costs of resilience in terms of new decision variables vector z in the expansion planning optimization problem. x and y are vectors used to model the binary and continuous variables for investment and operating decisions. f(x,y) is a set of constrained functions for investment and operation. g(x,z) is a new set of constraints related to resilience in the expansion planning model. The detailed formulation of the resilience-constrained IDNSEP according to (1)-(4) is provided in the continuation of this section. The objective function of the IDNSEP problem (5) is to simultaneously minimize the investment, operational, and resilience costs of networks in the planning horizon, which include nine terms. The terms related to the investment costs of new generation units, storage units, and distribution lines are modeled in (6), (7), and (8), respectively.

$$IC^{(n)}_{N,g,y} = (\frac{A}{P}, IR_\zeta, T^g) \sum_{g \in \Omega^{(n)}_{N,g}} x_{N,g,y} R_{N,g} C^I_{N,g} \tag{6}$$

$$IC^{(n)}_{N,s,y} = (\frac{A}{P}, IR_\zeta, T^s) \sum_{s \in \Omega^{(n)}_{N,s}} x_{N,s,y} R_{N,s} C^I_{N,s} \tag{7}$$

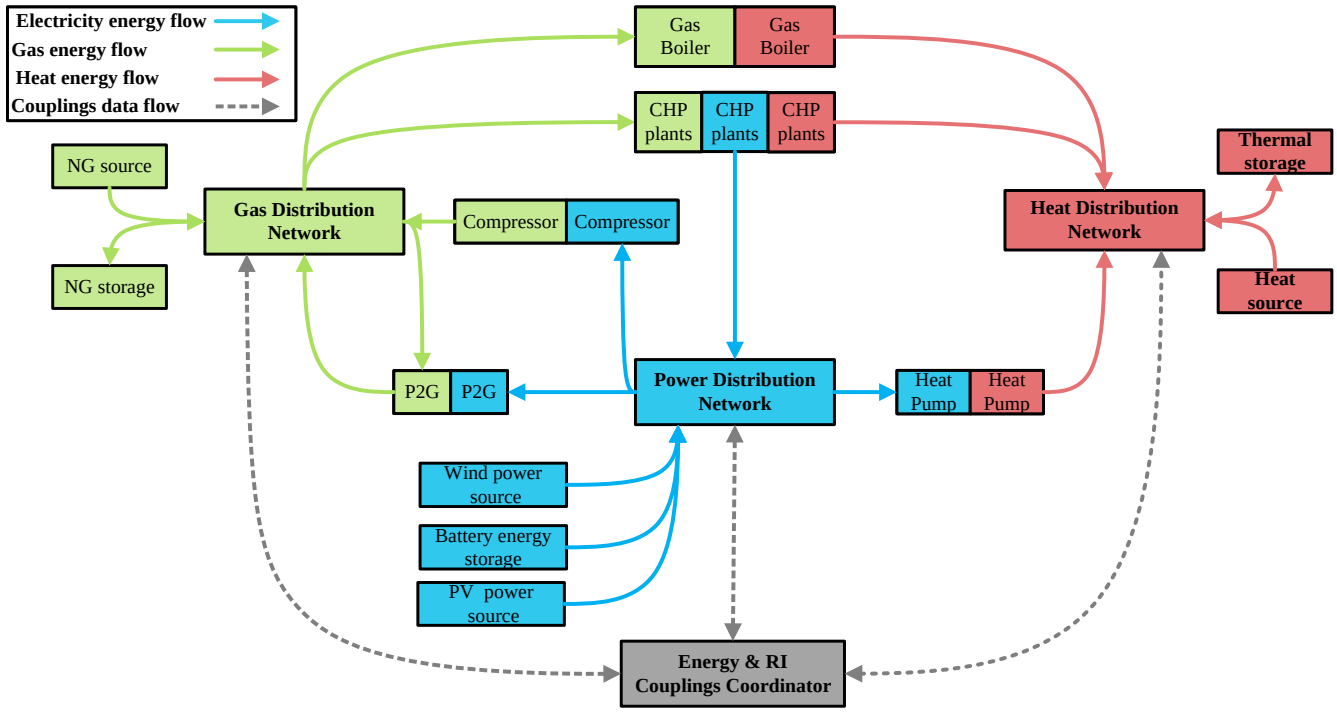

Figure 2: The proposed IDNs couplings and energy flow

$$Min\ C^{IDNSEP} = \min \sum_{\zeta} Pr_{\zeta} \left(\begin{array}{l} (\frac{P}{A}, IR_{\zeta}, T) \sum_{N \in \Omega_N} \sum_{y \in Y} (\frac{P}{F}, IR_{\zeta}, y)(IC^{(n)}_{N,g,y} + IC^{(n)}_{N,s,y} + IC^{(n,r)}_{N,L,y}) \\ + \sum_{N \in \Omega_N} \sum_{y \in Y} (\frac{P}{F}, IR_{\zeta}, y)(FOC^{(n,e)}_{N,g,y} + FOC^{(n,e)}_{N,s,y} + FOC^{(n,e)}_{N,L,y} + \sum_{s \in \Omega_s} N_s \sum_{t \in T_d} VOC_{N,y,s,t}{}^{n,e)}) \\ + \sum_{N \in \Omega_N} \sum_{y \in Y} (\frac{P}{F}, IR_{\zeta}, y) \sum_{s \in \Omega_s} N_s \sum_{t \in T_d} EP^{cost}_{N,y,s,t} \\ + \sum_{N \in \Omega_N} \sum_{y \in Y} (\frac{P}{F}, IR_{\zeta}, y) \sum_{N_H=0}^{5} \sum_{s \in \Omega_s} \rho^H_s N_H f^H N_H \sum_{t \in T_e} RI^{cost}_{N,y,s,t} \end{array} \right) \quad (5)$$

$$IC^{(n,r)}_{N,L,y} = (\frac{A}{P}, IR_{\zeta}, T^L) \sum_{L \in \Omega^{(n,e)}_{N,L}} (x_{N,L,y} L^n_N C^I_{N,L} + x_{E,L,y} L^r_E C^r_{E,L}) \quad (8)$$

where terms A, P, and F express annual value, present value and future value, respectively. The terms $(\frac{A}{P}, IR_{\zeta}, T)$, $(\frac{P}{A}, IR_{\zeta}, T)$, and $(\frac{P}{F}, IR_{\zeta}, T)$ are time value of money that converts an annual value to its equivalent present value, a present value to its equivalent annual value, and a future value to its equivalent present value with interest rate IR_{ζ} over time T, respectively and are calculated using the formulation provided in [9]. The investment costs for the distribution lines in (8) includes the cost for installation in the relevant distribution network, the new tie-lines for the reconfiguration in the PDN as well as lines to be reinforced in the PDN. Fixed operation costs of new and existing generation units, storage units, and distribution lines are presented in (9), (10), and (11), respectively. The variable costs are expressed in (12).

$$FOC^{(n,e)}_{N,g,y} = \sum_{g \in \Omega^{(n,e)}_{N,g,y}} R_{N,g,y} C^O_{N,g} \quad (9)$$

$$FOC^{(n,e)}_{N,s,y} = \sum_{s \in \Omega^{(n,e)}_{N,s}} R_{N,s,y} C^O_{N,s} \quad (10)$$

$$FOC^{(n,e)}_{N,L,y} = \sum_{L \in \Omega^{(n,e)}_{N,L}} L^{(n,e)}_{N,ij/kl/mr,y} C^O_{N,L} \quad (11)$$

$$VOC^{(n,e)}_{N,y,s,t} = \sum_{L \in \Omega^{(n,e)}_{N,g}} E_{N,g,y,s,t} C^{EC}_{N,g,y,s,t} \quad (12)$$

The purchasing energy cost from the upstream grid is modeled using (13). The last term in (5) models the resiliency cost, corresponding to the last term in (1) which is expressed in (14). Variable operating costs, costs of purchasing energy from the upstream grid, and resilience costs in (5) are seasonally calculated for the whole year. Instead of just considering a snapshot of the demand profile in the year, the seasonal variation in the demand and wind and solar power sources generation in the IDNs are also considered using seasonal profiles to increase the model's accuracy. In this way, in addition to avoiding the simulation complexity due to the calculations for all days, the model's accuracy also increases.

$$EP^{cost}_{N,y,s,t} = E_{N,slack,y,s,t} C^{EC}_{N,slack,y,s,t} \quad (13)$$

$$RI^{cost}_{N,y,\mathbb{s},t} = \sum_{i\in\Omega_f} (D^{NS}_{N,i,y,\mathbb{s},t} C^{retail}_{N,y,\mathbb{s},t} \Delta t + D^{NS}_{N,i,y,\mathbb{s},t} C^{LD}_{N,y,\mathbb{s},t} \Delta t + C^{repair}_{P} N^{FP}) \quad (14)$$

Resilience is defined at the distribution network level in this paper. The resilience cost in (14) consists of three terms, corresponding to unsupplied energy in the IDNs due to outage in the PDN, financial losses due to the lost load of IDNs customers, and imposed cost to the PDN due to poles and conductor failure, respectively. The latter of which is more related to reliability indices. However, in the technical view, a resilience index is used, which perfectly models the resilience of IDNs. In order to implement a reality-based model, real-time pricing (RTP) for energy carriers is considered. In this way, the IDNs have the opportunity to decide how to optimize their energy purchase costs and their energy utilization from time to time. Also, this model can result in optimal performance of coupling units in IDNs. For example, when the price of natural gas is high and the price of electricity is low; it is optimal to convert excess electricity into natural gas using P2G units. The hourly unsupplied energy cost in (14) is calculated using the RTP. It is customary to meet demand growth in the future, considering capacity expansion investment as a part of the national budget. This is taken into consideration within the proposed IDNSEP model under annual budget limit constraint (15) for IDNs.

$$\sum_{N\in\Omega_N} \left(\begin{array}{l} (IC^{(n)}_{N,g,y} + IC^{(n)}_{N,s,y} + IC^{(n,r)}_{N,L,y}) \\ +(FOC^{(n,e)}_{N,g,y} + FOC^{(n,e)}_{N,s,y} + FOC^{(n,e)}_{N,L,y}) \\ + \sum_{\mathbb{s}\in\Omega_{\mathbb{s}}} N_{\mathbb{s}} \sum_{t\in T_d} VOC^{(n,e)}_{N,y,\mathbb{s},t} \end{array} \right) \le C_{Budget} \quad (15)$$

2.2. Power distribution network model

AC power flow equations (16)–(19), limit on power exchange with the upstream grid (20), active and reactive power generation limits of power sources (21)-(22), line active and reactive power flow limit (23)-(25), voltage magnitude and angle constraints (26)-(27), power demand curtailment bounds (28) are operating constraints of power flow in the PDN. The non-linear constraints (20) is linearized using special-order sets of type 2 (SOS2) method according to [26]. Three types of power sources exist in the model associated with constraints (21) and (22), including CHPs, wind turbines (WTs) , and PV farms. P2G is a power consumer in the PDN and a source of gas production for the GDN.

$$\sum_{g\in\Omega_{E,g}} P_{E,i,g,t} - P^{D}_{E,i,t} - \sum_{s\in\Omega_{E,s}} (P^{ch}_{E,i,s,t} - P^{dis}_{E,i,s,t}) + P^{curt}_{E,i,t} = \sum_{\substack{j\in\Omega_{E,n} \\ i\neq j}} P_{E,ij,t} \quad (16)$$

$$\sum_{g\in\Omega_{E,g}} Q_{E,i,g,t} - Q^{D}_{E,i,t} + Q^{curt}_{E,i,t} = \sum_{\substack{j\in\Omega_{E,n} \\ i\neq j}} Q_{E,ij,t} \quad (17)$$

$$\sum_{j\in\Omega_{E,n}} P_{E,ij,t} = (2V_{i,t} - 1)G_{ii} + \sum_{\substack{j\in\Omega_{E,n} \\ j\neq i}} (\theta_{i,t} - \theta_{j,t})B_{ij} + \sum_{\substack{j\in\Omega_{E,n} \\ j\neq i}} (V_{i,t} + V_{j,t} - 1)G_{ij} \quad (18)$$

$$\sum_{j\in\Omega_{E,n}} \hat{Q}_{E,ij,t} = -(2V_{i,t} - 1)B_{ii} - \sum_{\substack{j\in\Omega_{E,n} \\ j\neq i}} (\theta_{i,t} - \theta_{j,t})G_{ij} - \sum_{\substack{j\in\Omega_{E,n} \\ j\neq i}} (V_{i,t} + V_{j,t} - 1)B_{ij} \quad (19)$$

$$(P^{Imp}_{E,t})^2 + (Q^{Imp}_{E,t})^2 \le (\overline{S}^{Imp}_{E,t})^2 \quad (20)$$

$$\underline{P}_{E,i,g} \le P_{E,i,g,t} \le \overline{P}_{E,i,g} \quad (21)$$

$$\underline{Q}_{E,i,g} \le Q_{E,i,g,t} \le \overline{Q}_{E,i,g} \quad (22)$$

$$P_{E,ij,t} = \Re(Z^{L}_{i,j})(V_{i,t} - V_{j,t}) - \Im(Z^{L}_{i,j})(\theta_{i,t} - \theta_{j,t}) \quad (23)$$

$$Q_{E,ij,t} = -\Im(Z^{L}_{i,j})(V_{i,t} - V_{j,t}) - \Re(Z^{L}_{i,j})(\theta_{i,t} - \theta_{j,t}) \quad (24)$$

$$P_{E,ij,t} + P_{E,ji,t} \le \overline{P}^{loss}_{E,ij} \quad (25)$$

$$\underline{V}_i \le V_{i,t} \le \overline{V}_i \quad (26)$$

$$\underline{\theta}_i \le \theta_{i,t} \le \overline{\theta}_i \quad (27)$$

$$0 \le P^{curt}_{E,i,t} \le P^{D,Ncr}_{E,i,t} \quad (28)$$

In distribution lines, power flow is limited by the maximum thermal capacity of the conductors. This constraint can be modeled with the maximum apparent power of the line. Based on [33], it can be converted to the line power losses as expressed in (25), which is a linear constraint and is superior to the nonlinear model in terms of reducing the complexity of the model. The demand curtailment constraint in (28) is applied to non-critical demands in emergency conditions if needed. The GDN and DHN demands that are supplied from the PDN's buses such as pumps and electric boilers in the DHN and compressor in the GDN are critical loads. The battery energy storage system (BESS) constraints are modeled in (29)-(32). The state-of-charge (SoC) of BESS at each time instant is represented by (29) and limited through constraints (30). Limits on charge and discharge power of the BESS are shown in (31) and (32), respectively. The initial SoC of the BESS units is considered as 0.5.

$$SoC_{E,s,t} = SoC_{E,s,t-1} + \frac{\eta^{ch}_{E,s} P^{ch}_{E,i,s,t}}{\overline{P}_{E,s}} - \frac{P^{dis}_{E,i,s,t}}{\eta^{dis}_{E,s} \overline{E}_{P,s}} \quad (29)$$

$$\underline{SoC}_{E,s} \le SoC_{E,s,t} \le \overline{SoC}_{E,s} \quad (30)$$

$$0 \le P^{ch}_{E,s,t} \le \overline{P}^{ch}_{E,s} x_{E,s,t} \quad (31)$$

$$0 \le P^{dis}_{E,s,t} \le \eta^{dis}_{E,s} \overline{P}^{dis}_{E,s} (1 - x_{E,s,t}) \quad (32)$$

2.3. Gas distribution network model

The main components in the GDNs consist of the town board stations (TBSs), pipelines, compressor stations, valves, regulators, natural gas storage (GS), and demand. Many of the parameters that affect the gas flow through

pipelines, such as the pressure of the nodes, natural gas type, and the pipeline's length and diameter, are fixed in the daily operation of GDNs. The GDN steady-state modeling is described below. Nodal mass balance and gas flow in pipelines of the GDN are modeled as (33) and (34), respectively.

$$\sum_{g\in\Omega_{G,g}} q_{G,k,g,t} - q^{D}_{G,k,t} - \sum_{s\in\Omega_{G,s}} (q^{ch}_{G,k,s,t} - q^{dis}_{G,k,s,t}) + q^{curt}_{G,i,t} = \sum_{\substack{j\in\Omega_{G,n}\\ k\neq l}} q_{G,kl,t} \tag{33}$$

$$q^{2}_{G,kl,t} = sign(q_{G,kl,t})\psi^{2}_{G,kl}(\Gamma_{G,k,t} - \Gamma_{G,l,t}) \tag{34}$$

For simplicity and computational efficiency, the quadratic term on the left side of (34) is approximated using the piecewise linearization method (details can be found in [34]). Constraints (35)-(37) sets the bounds on the gas production of gas sources, gas flow in pipelines, and gas pressure in nodes.

$$\underline{q}_{G,k,g} \le q_{G,k,g,t} \le \overline{q}_{G,k,g} \tag{35}$$

$$\underline{q}_{G,kl} \le q_{G,kl,t} \le \overline{q}_{G,kl} \tag{36}$$

$$\underline{\Gamma}_{G,k} \le \Gamma_{G,k,t} \le \overline{\Gamma}_{G,k} \tag{37}$$

Constraint (38) represents the maximum possible demand curtailment in the GDN. Demand curtailment can be applied to non-critical gas demands only. Natural gas-consuming units in the PDN and DHN are considered critical gas demands.

$$0 \le q^{curt}_{G,k,t} \le \overline{q}^{D,Ncr}_{G,k,t} \tag{38}$$

The Gas Compressor compensates for the pressure loss of gas pipelines for long-distance transmissions. Gas pressure constraint for active pipelines with compressor is given in (39).

$$\Gamma_{G,k,t} \le \Gamma_{G,l,t} \le \xi_{kl}\Gamma_{G,k,t} \tag{39}$$

It is assumed that when the compressor input power is cut off or reduced, it operates as a regular pipeline. When the compressor operates as a regular pipeline, the compression coefficient, ξ_{kl}, is equal to 1. The GS mathematical model is addressed by (40)-(43) which SoC in consecutive time stages of the problem, the SoC level limit of the GS, and charge and discharge mass flow rate limits are expressed, respectively.

$$SoC_{G,s,t} = SoC_{G,s,t-1} + \frac{\eta^{ch}_{G,s} q^{ch}_{G,k,s,t}}{\overline{q}_{G,s}} - \frac{q^{dis}_{G,k,s,t}}{\eta^{dis}_{G,s}\overline{q}_{G,s}} \tag{40}$$

$$\underline{SoC}_{G,s} \le SoC_{G,s,t} \le \overline{SoC}_{G,s} \tag{41}$$

$$0 \le q^{ch}_{G,s,t} \le \overline{q}^{ch}_{G,s} x_{G,s,t} \tag{42}$$

$$0 \le q^{dis}_{G,s,t} \le \eta^{dis}_{G,s}\overline{q}^{dis}_{G,s}(1 - x_{G,s,t}) \tag{43}$$

2.4. District heating network model

Water is the medium in the DHNs and, heat transfers energy between two nodes in these networks. Two parameters play a key role in the operation mode of DHNs: temperature and mass flow. Regarding control of these parameters, there are four types of operating strategies for a DHN [34]. To have the most economical and accurate design, the variable temperature-variable flow (VT-VF) operating strategy is employed in this paper. The nodal mass balance and water flow equations of the DHN are modeled as follows:

$$\sum_{g\in\Omega_{H,g}} M_{H,m,g,t} - M^{D}_{H,m,t} - \sum_{s\in\Omega_{H,s}} (M^{ch}_{H,m,s,t} - M^{dis}_{H,m,s,t}) + M^{curt}_{H,m,t} = \sum_{\substack{r\in\Omega_{H,n}\\ m\neq r}} c^{w} m_{H,ij,t}(\tau^{in}_{H,mr,t} - \tau^{out}_{H,mr,t}) \tag{44}$$

$$m^{2}_{H,mr,t} = sign(m_{H,mr,t})\psi^{2}_{H,mr}(\Pi_{H,m,t} - \Pi_{H,r,t}) \tag{45}$$

The squared pressure value is used in (45) to eliminate the nonlinearity of the "Weymouth equation". The quadratic term on the left side is approximated using the piecewise linearization method. The water temperature is the state parameter that measures thermal energy. Heat loss between hot water in the pipeline and the ambient temperature is modeled by (46) and the nodal temperature of the mixed water is calculated by (47) as done in [35]. As expressed in (48) the temperature of mass flowing out of the pipeline is equal to the mixed temperature at the start node. To simplify the problem, the heat loss coefficient φ_{mr} is assumed to be a constant for simplicity.

$$(\tau^{out}_{H,mr,t} - \tau^{a}) = (\tau^{in}_{H,mr,t} - \tau^{a})\varphi_{mr} \tag{46}$$

$$\tau^{mix}_{H,r,t} \sum_{mr\in\Omega_{H,L}} m_{H,mr,t} = \sum_{ij\in\Omega_{H,L}} (m_{H,mr,t}\tau^{out}_{H,mr,t}) \tag{47}$$

$$\tau^{in}_{H,mr,t} = \tau^{mix}_{H,r,t} \;\forall m, r \in \Omega_{H,n}\;,\; mr \in \Omega_{H,L}\;,\; t \in T \tag{48}$$

Constraints corresponding to the upper and lower limits of mass flow in heat sources, nodes water pressure and temperature are expressed by (49)-(51).

$$\underline{m}_{H,m,g} \le m_{H,m,g,t} \le \overline{m}_{H,m,g} \tag{49}$$

$$\underline{\Pi}_{H,m} \le \Pi_{H,m,t} \le \overline{\Pi}_{H,m} \tag{50}$$

$$\underline{\tau}_{H,m} \le \tau_{H,m,t} \le \overline{\tau}_{H,m} \tag{51}$$

Constraint (52) represents the maximum possible demand curtailment in the DHN. Demand curtailment can be applied to non-critical heat demands only.

$$0 \le M^{curt}_{H,m,t} \le \overline{M}^{D,Ncr}_{H,m,t} \tag{52}$$

The thermal storage (TS) mathematical model is expressed in (53)-(56), which is similar to the BESS and GS models.

$$SoC_{H,s,t} = SoC_{H,s,t-1} + \frac{\eta^{ch}_{H,s} M^{ch}_{H,m,s,t}}{\overline{M}_{H,s}} - \frac{M^{dis}_{H,m,s,t}}{\eta^{dis}_{H,s}\overline{M}_{H,s}} \tag{53}$$

$$\underline{SoC}_{H,s} \le SoC_{H,s,t} \le \overline{SoC}_{H,s} \tag{54}$$

$$0 \le M^{ch}_{H,s,t} \le \overline{M}^{ch}_{H,s} x_{H,s,t} \tag{55}$$

$$0 \le M^{dis}_{H,s,t} \le \eta^{dis}_{H,s} \overline{M}^{dis}_{H,s} (1 - x_{H,s,t}) \tag{56}$$

2.5. Coupling component model

In this paper, CHP, P2G, WP, compressor, EB, and GB couples IDNs. Among these, CHP plays the most significant role in coupling between IDNs. The relationship between heat production and electrical power generation of CHP units is expressed in (57) [36], while (58) depicts the natural gas fuel consumption of CHP [37].

$$M_{i,g,t} = P_{E,i,g,t} \frac{1 - \eta^{CHP,e}_{i,g} - \eta^{CHP,hl}_{i,g}}{\eta^{CHP,e}_{i,g} \beta^{CHP}_{i,g}}$$
$$\forall i \in \Omega^{CHP}_{E,n} \ , \ g \in \Omega_{CHP} \ , \ t \in T \tag{57}$$

$$q^{D,CHP}_{G,i,t} = \eta^{CHP,e}_{i,g} P_{E,i,g,t}$$
$$\forall i \in \Omega^{CHP}_{E,n} \ , \ g \in \Omega_{CHP} \ , \ t \in T \tag{58}$$

Another component that creates direct coupling between the GDN and the PDN is P2G. The relationship between power consumption and gas produced by the P2G units is modeled using (59).

$$q_{E,i,t} = \eta^{P2G}_{i,g} P^{D,P2G}_{E,i,t} \ \ \forall i \in \Omega^{P2G}_{E,n} \ , \ g \in \Omega_{P2G} \ , \ t \in T \tag{59}$$

where $\eta^{P2G}_{i,g}$ is the conversion coefficient of electric energy to natural gas based on [37]. Similarly, the energy conversion in electric and gas boilers, coupling the PDN and GDN to the DHN, are modeled by (60)-(63).

$$M_{H,m,g,t} = \eta^{EB}_{m,g} P^{D,EB}_{E,m,t} \ \ \forall m \in \Omega^{EB}_{H,n} \ , \ g \in \Omega_{EB} \ , \ t \in T \tag{60}$$

$$0 \le P^{D,EB}_{E,m,t} \le \overline{P}^{D,EB}_{E,m} \tag{61}$$

$$M_{H,m,g,t} = \eta^{GB}_{m,g} q^{D,GB}_{G,m,t} \ \ \forall m \in \Omega^{GB}_{H,n} \ , \ g \in \Omega_{GB} \ , \ t \in T \tag{62}$$

$$0 \le q^{D,GB}_{G,m,t} \le \overline{q}^{D,GB}_{G,m} \tag{63}$$

According to (61) and (63), the EB power consumption and the GB gas consumption are limited. Natural gas compressors are installed along gas pipelines to compensate for gas pressure drop. The compressor increases the pressure of a gas by reducing its volume using power consumption. Compressor power consumption during compression is modeled by (64) according to [37].

$$P^{D,GC}_{G,k,t} = q_{G,c,t} k_1 \frac{k_2}{1 - k_2} \left(\left(\frac{\Gamma_{l,t}}{\Gamma_{k,t}}\right)^{0.5 \frac{k_2}{1-k_2}} - 1 \right)$$
$$\forall k, l \in \Omega^{Co}_{G,n} \ , \ Co \in \Omega_{G,Co} \ , \ t \in T \tag{64}$$

The compressor's power consumption is related to the output and input pressure ratio and the mass flow through the compressor. The mass flow through the compressor is limited by (65). According to (66), the pressure ratio between the compressor's output and input is determined, which is limited by the possible operation range of the compressor.

$$\underline{q}_{G,k} \le q_{G,k,t} \le \overline{q}_{G,k} \ \ \forall k \in \Omega^{Co}_{G,n} \ , \ Co \in \Omega_{G,Co} \ , \ t \in T \tag{65}$$

$$\underline{CR} \le \left(\frac{\Gamma_{l,t}}{\Gamma_{k,t}}\right) \le \overline{CR} \tag{66}$$

Since the steady-state condition is studied in this paper, the transient behavior of the compressor during the fault is not considered. Therefore, the compressor acts as a regular pipeline when an outage in the PDN leads to a cut-off or reduction in the compressor input power. The WP in the DHN is used to compensate for water pressure losses in pipelines. The power consumption of the WP is modeled by (67) based on [35], which is limited by technical constraint (68).

$$P^{D,WP}_{H,m,t} = \frac{m_{H,WP,t} (\Pi^{out}_{H,m,t} - \Pi^{in}_{H,m,t})}{\eta^{WP} \rho^{w}}$$
$$\forall m \in \Omega^{WP}_{H,n} \ , \ WP \in \Omega_{WP} \ , \ t \in T \tag{67}$$

$$\underline{P}^{D,WP}_{H,m} \le P^{D,WP}_{H,m,t} \le \overline{P}^{D,WP}_{H,m}$$
$$\forall m \in \Omega^{WP}_{H,n} \ , \ WP \in \Omega_{WP} \ , \ t \in T \tag{68}$$

where in (67), $m_{H,WP,t}$ is the water flow through the pump. With the help of the LADMMPSAP, coupling variables exchange between IDNs while maintaining the independence of operation of each distribution network.

2.6. Formulation of stage 2 objective function

The proposed RI for the IDNs is expressed in (69), which is a normalized index for evaluating the resilience of IDNs. The RI should picture the system's resilience in the whole disruption and recovery phases. The proposed RI includes both phases as follows:

$$RI_t = \sum_{N \in \Omega_N} \omega_N \left(\frac{\sum_{t_d}^{t_{pr}} D^{nor}_{N,t}}{D^{nor}_{N,t_d} (t_{pr} - t_d)} \right) \tag{69}$$

where ω_N is the importance weight of network N such that $\sum_{N \in \Omega_N} \omega_N = 1$. $D^{nor}_{N,t}$ represents the normalized demand of network N at time t, which is obtained by dividing the supplied demand by scheduled demand. The proposed RI is normalized; the higher its value, the more resilient the system is. $(t_{pr} - t_d)$ is a measure of system stamina during the disruption phase and quality of operation in the recovery phase. Therefore, the RI measures the dynamic behavior of the system in response to a disturbance. After a hurricane, the PDN forms islands to supply the demands disrupted from the upstream grid. Therefore, new constraints are proposed to guarantee the PDN radiality. The operational constraints of the PDN in 2.2 should be reformulated considering formed islands resulting from the line outages under hurricanes which is done using the presented method in [38]. The reconfiguration of the PDN considering candidate tie-lines is included in the reformulation based on [39],

in which radiality is guaranteed using the spanning-tree method. The detail of the reconfiguration formulation can be found in [39]. Stage 2 model is defined for the emergency condition with time interval $T_e = [t_d, t_{pr}]$. Investigation of resilience impacts in the IDN's expansion planning is a sub-module. Therefore, to simplify the problem and consider the pessimistic condition (due to being in the peak load time interval), it is assumed that the hurricane incident will occur in the period of 16:00 to 21:00 during the planning period. It is also assumed that repairing damaged lines takes three hours. Optimization problem (70) includes optimal recovery measurements to maximize the proposed RI in the emergency condition. Given that the resilience improvement objective is studied from a planning perspective in this study, some simplification assumptions have been applied to the stage 2.

$$OF_2 = \max \sum_{\nu} Pr(\nu) RI_{t|\nu}$$
$$= \max \sum_{N \in \Omega_N} \sum_{\nu} Pr(\nu) \omega_N \left(\frac{\sum_{t_d}^{t_{pr}} D_{N,t}^{nor}}{D_{N,t_d}^{nor}(t_{pr} - t_d)} \right) \quad (70)$$

where ν is a set of wind profile speed scenarios with different classes according to the Saffir-Simpson category. Post-hurricane recovery strategy's effectiveness depends on accurately estimating risks incurred due to induced damage to the system. By integrating the cost associated with outages induced by various damage scenarios over the probabilities of these scenarios, imposed risk can be computed. Because pipelines are primarily located underground, they are protected from the direct effects of a hurricane in the GDN and DHN. Therefore, this paper focuses on the hurricane wind-induced damage to PDN's overhead infrastructural assets. The damages are dependent on the hurricane wind speed, direction, and duration. Wind turbines are vulnerable to hurricanes since the maximum wind speeds can exceed the cut-off speed limits (usually 25-30 m/s) of wind turbines. Furthermore, because the reliable forecast of when the wind turbine shuts down due to critical speeds over the hurricane is impossible, it is assumed that wind turbines shut down in emergency conditions in stage 2. In the case of PDN's overhead lines, the situation is different because the vulnerability of this component is a probable event and is computed based on the fragility curve. These curves indicate the probability of component failure for different wind speeds. The disruption phase modeling consists of two steps, first extracting the hurricane model and then computing the probability of PDN's line failure in different hurricane scenarios. A simple axisymmetric hurricane track is considered, which moves a straight line with a constant translation speed. Locations of the PDN's components are defined using a 2D vector determining latitude and longitude of components.The lack of probabilistic spatially-time varying models for infrastructure outage prediction in PDNs is tangible in the literature. The well-known Holland model [40] is used to compute the hurricane wind speed at time t in location c with (71). The speed $v_{c,t}$ is a function of $r_{c,t}$, the radial distance of location c from the hurricane center, which is assumed to be at the center point of the PDN. Holland's model has three parameters: maximum wind speed, $V_{\max}$, the radius of winds, $R_{\max}$, and the shape of the hurricane, α, (More details can be found in [36]).

$$v_{c,t} = V_{\max} \left(\frac{R_{\max}}{r_{c,t}} \right)^{\alpha/2} \exp^{(0.5(1-(\frac{R_{\max}}{r_{c,t}})^{\alpha}))} \quad (71)$$

The overall failure probability of an overhead line under wind speed $v_{c,t}$ is modeled using (72) considering poles and conductor failures [41]-[42]. The fragility curve of poles and conductors, which is a function of wind speed and structural characteristics of these components, is calculated using the log-normal distribution function according to [22].

$$P_L^f(v_{c,t}) = 1 - \prod_u [1 - P_{Po_u}^f(v_{c,t})] \prod_w [1 - P_{Co_w}^f(v_{c,t})] \quad (72)$$

Priority of strategies in stage 2 is sorted using the proposed RII in (73), which integrates stage 2 with the main planning problem in the stage 1.

$$RII_t^L = \frac{RI_{(t|Pr(F_L)=0)}}{RI_t} \ \forall L \in \Omega_{E,L}^f \ ,$$
$$\Omega_{E,L}^f = \{L | P_L^f > P_{Th}^f\} \ , \ t \in T_e \quad (73)$$

$$RII_t^{TL} = \frac{RI_{(t|x_{E,i,L,y}=1)}}{RI_t} \ \forall L \in \Omega_{TL} \ , \ t \in T_e \quad (74)$$

where RI_t is the optimal resilience of the IDNs at time t and $RI_{(t|Pr(F_L)=0)}$ is the optimal resilience of the IDNs at time t when the distribution line L is reinforced, and the failure probability is zero. So, RII_t^L measures the impact of a specific line reinforcement on the resilience of the IDNs. Similarly, RII_t^L measures the potential impact of a specific tie-line installation on the resilience of the IDNs where $RI_{(t|x_{E,i,L,y}=1)}$ is the optimal resilience of IDNs at time t when the tie-line L is installed in the PDN. In other words, two options for resilience improvement are evaluated using the proposed RII. First, PDN's lines reinforcement value (lines with more probability of failure than the threshold). Second, the importance of candidate tie-lines presence in hurricane scenarios. The priority of reinforcement and tie-line installation strategies sends to stage 1 of the IDNSEP as shown in Fig. 1.

3. Solution methodology

The ADMM fits convex problems with separable objective functions and linear constraints. The main advantage of the ADMM is that it converts the original problems to simpler sub-problems. Therefore, the centralized IDNSEP problem can be converted to decentralized sub-problems causing solving problems simpler and increasing the convergence speed. Linear ADMM, which is the so-called LADMM, is the linear version of ADMM, which makes solving the sub-problems even simpler. The ADMM or LADMM can be used for only two blocks of variables, while the proposed IDNSEP problem in this paper integrates

three distribution networks with three blocks of variable and therefore LADMM with Parallel Splitting and Adaptive Penalty (LADMMPSAP) is used which fits for more than two blocks of variables [32]. LADMMPSAP updates variables parallel instead of serial, and thus convergence can still be guaranteed. Also, using the adaptive penalty in LADMMPSAP helps faster convergence. The introduced modified LADMMPSAP in this paper has been stemmed from form [32], where a new stop criterion is added to ensure that in each iteration $C_{N,t}^{sep((\kappa))}$ improves and also the variable updating process is improved. The difference of $x_r^{(\kappa)}$ from $x_{r'}^{(\kappa)}$ is used in the variable updating process instead of using $A(\lambda^{(\kappa)})$ (A is a linear mapping for the problem constraints). These modifications help to a faster and more reliable algorithm's convergence. The general centralized IDNSEP model of (1)-(4) which the objective function and constraints are defined in detail in (5)-(74), is reformulated using the LADMMPSAP as a linearly constrained separable convex problem. To that end, each distribution network tackles its own decoupled optimization problem. RECU collects relevant information from IDNs and sends it to them. The three separated minimization problems in the decentralized IDNSEP model for the PDN, GDN, and DHN are presented in (75), (76), and (77), respectively. Where in (75), $C_{E,t}^{sep(\kappa)}$ includes the total investment, operation, energy purchase, and resilience costs for the PDN, and costs related to the GDN and DHN are not included. In the PDN sub-problem, $q_{E,\hat{j}i,t}^{(\kappa+1)}$ is variable while $q_{G,\hat{j}i,t}^{(\kappa)}$ is supposed to be a constant determined by the consensus of gas system operator and RECU and vice versa $q_{G,\hat{j}i,t}^{(\kappa+1)}$ is variable in the GDN subproblem, and $q_{E,\hat{j}i,t}^{(\kappa)}$ is supposed constant, which is determined through consensus of the PDN and coordinator unit. Similarly, variables and parameters are specified in decomposed sub-problems. A repetitive process minimizes the differences between these variable and constant parameters in each subproblem. The LADMMPSAP algorithm is described in Algorithm I which is shown in Appendix. A, using Lagrangian multipliers δ, penalty factors λ, and termination thresholds ε. At each iteration of the problem-solving process, objective functions of both stages are calculated. A fuzzy decision method is used to select the optimal solution from the solutions provided by the two-stage IDNSEP problem-solving. A linear membership function is defined by (78), which indicates the optimality degree of solution in κ-th iteration.

$$M^{\kappa} = \begin{cases} 0 & \text{if } OF^{\kappa} < OF^{min} \\ \frac{OF^{\kappa} - OF^{min}}{OF^{max} - OF^{min}} & \text{if } OF^{min} \le OF^{\kappa} \le OF^{max} \\ 1 & \text{if } OF^{\kappa} > OF^{max} \end{cases} \quad (78)$$

The optimal solution is determined using (79), which selects the minimum member function in (78).

$$M^{min} = \min\{M^{\kappa}\} \ \ \forall \kappa \quad (79)$$

The proposed methodology solution framework is illustrated as the flowchart in Fig. 3. The flowchart expresses the process of forming and solving the proposed two-stage IDNSEP in the form of three sequential sections. Section A presents the process of forming the two-stage IDNSEP model. As seen in the steps of this section, the centralized model is first formed, and then the model is linearized and is converted to decentralized one using LADMMPASP method, creating the proposed two-stage IDNSEP in this paper. The blue arrow indicates the connection between sections A and B, and the solution of stage 1 of the two-stage IDNSEP begins in Section B. Section B presents the step-by-step problem-solving process, which depends on the outputs of stage 2. This connection is indicated by the "call Section C" rectangular box in Section B. Section C is responsible for solving the problem of stage 2, the solution process specified in this Section. The outputs of Section C are called in Section B to solve the Stage 1 problem. Also, the black arrow from Section B to Section C indicates sending updated strategies at each iteration of the Stage 1 problem to Stage 2 for the next iteration. The global procedure of modeling can be summarized as the following steps:

Step 1 (Uncertainty modeling): load growth, wind generation output, PV generation output, and interest rate are the sources of uncertainty in the proposed model. These uncertainties are considered to generate scenarios with associated probabilities in Table. 1 to define a stochastic expansion planning problem model. The hurricane scenarios defined in Section C of the flowchart are used to calculate component failure probabilities.

Step 2 (Centralized IDNSEP modeling): First, resilience-based modeling of the IDNSEP objective function is established, and then each distribution network is modeled using operation constraints separately. The resulting model is a mixed-integer nonlinear problem (MINLP) which, due to the size of the problem, solving will be sophisticated computationally.

Step 3 (Coupling modeling and linearization): To determine the connections between IDNs, coupling equations are expressed in (57)-(68). The linearization methods of each nonlinear equation is expressed in the related section.

Step 4 (Equivalent reformulation): The constructed model in the previous steps is a centralized model, which is a complicated one. Using the LADMMPSAP, the centralized model is reformulated as a model with the separated sub-problems in (75)-(77) causing problem-solving simpler and speeds up convergence.

Step 5 (Solution): Solving procedure is shown in Section B and Section C of the flowchart. The reinforcement and reconfiguration strategies set are generated and updated in Section C, and the results are used in section B. In each year, reinforcement and reconfiguration, strategies are generated considering the hurricane scenario in that year, and the results are as the updated inputs in Section B. After executing the problem solving loops for each year iteration, the results of that year will be sent to Section C to update the network input parameters for the following year's iteration loop.

$$OF_1^E = \min \sum_{\zeta} Pr_{\zeta}$$

$$\left(\begin{array}{l} C_{E,t}^{sep(\kappa)} + \sum_{\hat{k}i}(\delta_{\hat{k}i,1}^{(\kappa)}(q_{G,\hat{k}i,t}^{(\kappa)} - q_{E,\hat{k}i,t}^{(\kappa+1)}) + \frac{\lambda_1^{(\kappa)}}{2}\|q_{G,\hat{k}i,t}^{(\kappa)} - q_{E,\hat{k}i,t}^{(\kappa+1)}\|_2^2) \\ + \sum_{i\hat{m}}(\delta_{im,2}^{(\kappa)}(P_{E,i\hat{m},t}^{(\kappa+1)} - P_{H,i\hat{m},t}^{(\kappa)}) + \frac{\lambda_2^{(\kappa)}}{2}\|P_{E,i\hat{m},t}^{(\kappa+1)} - P_{H,i\hat{m},t}^{(\kappa)}\|_2^2) + \sum_{i\hat{k}}(\delta_{ik,3}^{(\kappa)}(P_{E,i\hat{k},t}^{(\kappa+1)} - P_{G,i\hat{k},t}^{(\kappa)}) + \frac{\lambda_3^{(\kappa)}}{2}\|P_{E,i\hat{k},t}^{(\kappa+1)} - P_{G,i\hat{k},t}^{(\kappa)}\|_2^2) \end{array} \right) \tag{75}$$

$$OF_2^G = \min \sum_{\zeta} Pr_{\zeta}$$

$$\left(\begin{array}{l} C_{G,t}^{sep(\kappa)} + \sum_{\hat{k}i}(\delta_{\hat{k}i,1}^{(\kappa)}(q_{G,\hat{k}i,t}^{(\kappa+1)} - q_{E,\hat{k}i,t}^{(\kappa)}) + \frac{\lambda_1^{(\kappa)}}{2}\|q_{G,\hat{k}i,t}^{(\kappa+1)} - q_{E,\hat{k}i,t}^{(\kappa)}\|_2^2) \\ + \sum_{i\hat{k}}(\delta_{ik,3}^{(\kappa)}(P_{E,i\hat{k},t}^{(\kappa)} - P_{G,i\hat{k},t}^{(\kappa+1)}) + \frac{\lambda_3^{(\kappa)}}{2}\|P_{E,i\hat{k},t}^{(\kappa)} - P_{G,i\hat{k},t}^{(\kappa+1)}\|_2^2) + \sum_{\hat{k}m}(\delta_{km,4}^{(\kappa)}(q_{G,\hat{k}m,t}^{(\kappa+1)} - q_{H,\hat{k}m,t}^{(\kappa)}) + \frac{\lambda_4^{(\kappa)}}{2}\|q_{G,\hat{k}m,t}^{(\kappa+1)} - q_{H,\hat{k}m,t}^{(\kappa)}\|_2^2) \end{array} \right) \tag{76}$$

$$OF_1^H = \min \sum_{\zeta} Pr_{\zeta}$$

$$\left(\begin{array}{l} C_{H,t}^{sep(\kappa)} + \sum_{i\hat{m}}(\delta_{im,2}^{(\kappa)}(P_{E,i\hat{m},t}^{(\kappa)} - P_{H,i\hat{m},t}^{(\kappa+1)}) + \frac{\lambda_2^{(\kappa)}}{2}\|P_{E,i\hat{m},t}^{(\kappa)} - P_{H,i\hat{m},t}^{(\kappa+1)}\|_2^2) \\ + \sum_{\hat{k}m}(\delta_{km,4}^{(\kappa)}(q_{G,\hat{k}m,t}^{(\kappa)} - q_{H,\hat{k}m,t}^{(\kappa+1)}) + \frac{\lambda_4^{(\kappa)}}{2}\|q_{G,\hat{k}m,t}^{(\kappa+1)} - q_{H,\hat{k}m,t}^{(\kappa+1)}\|_2^2) \end{array} \right) \tag{77}$$

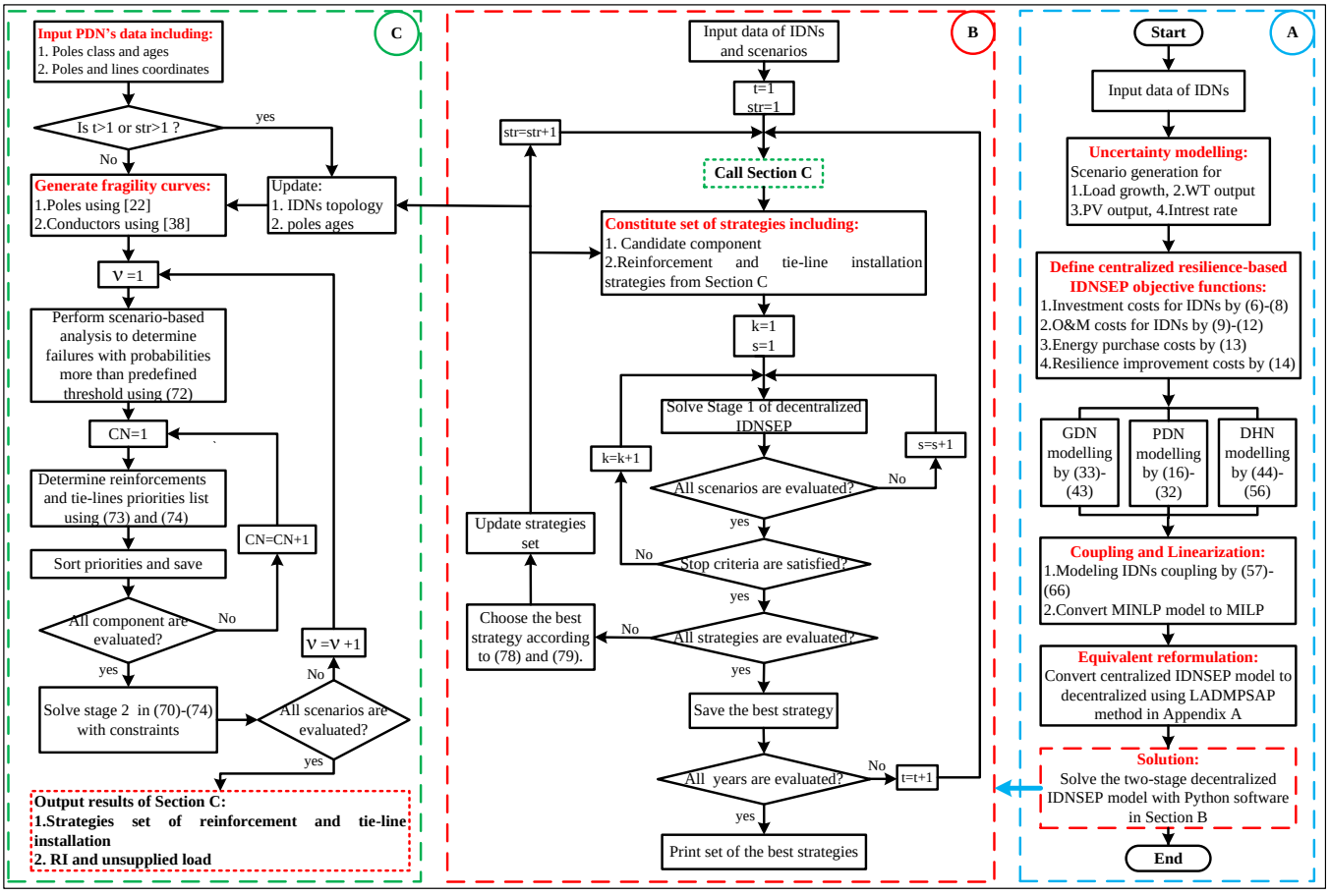

Figure 3: The proposed IDNSEP flowchart

4. Case studies and simulations

To express the effectiveness of the proposed resilience-constrained IDNSEP, the modified well-known IEEE 33-bus radial PDN [43] coupled with a 20-node GDN [44] and a 16-node DHN, as shown in Fig. 4, are studied. In all three networks, bus/node one is considered the slack bus. Existing networks include a 1.5 MW CHP in bus 5 and a 1 MW WT in bus 16 of the PDN, a 1500 m^3 TBS in node 8 of GDN and, a 1 MW GB in node 15 of DHN. Candidate alternative components, feeders, pipeline options for investment in the distribution networks, and candidate

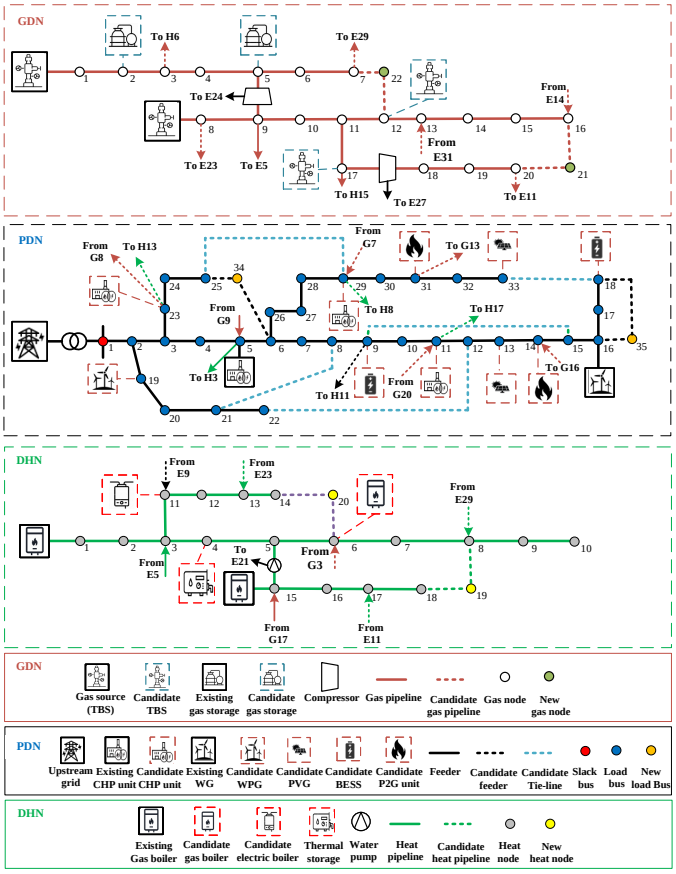

Figure 4: Integrated distribution networks schematic

points of coupling between these networks are shown. The rated capacities for CHPs, PV farms, wind turbine (WT), P2Gs, and BESSs in the PDN are considered as the sets of $\{0.6, 1, 1.2\}$, $\{1\}$, $\{1, 1.2\}$, $\{0.6, 1\}$, $\{0.6, 0.8, 1\}$ all in MW, respectively. The rated capacities of candidate TBSs are considered in the range of 500-2000 m^3 with a step size of 500 m^3 while for the candidate GSs the range of 1000-1500 m^3 with a step size of 100 m^3 is considered. The rated capacities for candidate generation and storage units in the DHN are considered in the range of 1-1.5 MW with a step size of 0.1 MW. The DHN is considered according to the PDN and GDN scale. The IDNs technical data is provided in Appendix. B. All of the lines in the PDN are overhead distribution lines, and the distance between the feeder's poles is assumed to be 100 meters. The PDN and GDN load profile are scaled to suit the proposed planning problem case requirements. The total load profile of the PDN includes fixed load and curtailable load that can be shed in emergency conditions. It is assumed that maximum 10% of the hourly loads are curtailable. The three study cases mentioned below are employed to evaluate the model comprehensively.

Case 1: IDNSEP without reconfiguration and reinforcement

Case 2: IDNSEP with reconfiguration-without reinforcement

Case 3: IDNSEP with reconfiguration and reinforcement

The budget limit for the centralized IDNSEP is \$ 3.5 million

Table 1
Scenarios of stage 1

Sce.	Prob.	Wind(%)	PV(%)	IR(%)	LG(%)
1	0.28	50	100	5	3
2	0.23	75	75	10	5
3	0.41	50	50	5	4
4	0.08	100	50	15	6

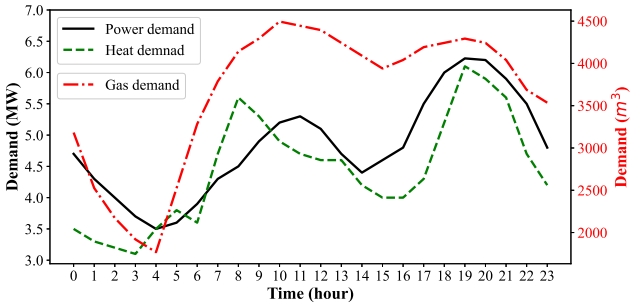

Figure 5: Demand profiles of the IDNs in the first year

per year, of which \$ 2 million, \$ 1 million, and \$ 0.5 million per year, respectively, are allocated to PDN, GDN, and DHN in the decentralized IDNSEP. Table. 1 shows the uncertainty scenarios with associated probabilities in stage 1. Wind and PV power generation, load growth (LG), and interest rate (IR) are considered sources of uncertainty in the model. Generation profiles of wind and solar power sources have been extracted for selected area of the study from [45], representing the nominal generation of wind and PV sources. A multi-level probabilistic model for wind and PV sources output power according to [9] is used to assign a probability to each output power level. Load growth of 3%, 4%, 5%, and 6% based on the historical data for load growth within the understudied area (Florida state in the USA) are considered in the modeling. It is assumed that load growth in the IDNs has the same pattern. Similarly, for interest rates, according to the economic reports, interest rates of 5%, 10%, 15% have been considered. Thus, 192 scenarios were created, which were reduced to 4 as presented in Table. 1, using the step-by-step scenario reduction method [46]. Fig. 5 shows the hourly demand profile of the IDNs in the first year of the study. The GDN demand in cubic meters per hour is observed in the second vertical axis on the right side of the diagram. For the better investigating impact of seasonal demand variation, a seasonal coefficient, according to Table. 2, is considered, which multiplies the peak demand profile in each season for demand profile adjustment in different seasons. Fig. 6 and 7 show the wind and solar power generation profiles in different seasons of the year, respectively. The middle day of each season is selected for deriving seasonal profiles based on the year 2019 data in [42]. These profiles show the generation per MW for wind and solar power sources in the understudied area. The understudy area is assumed to

Table 2
Seasonal demand coefficients

Network	Season			
	Spring	Summer	Fall	Winter
PDN	0.85	1	0.85	0.80
GDN	0.80	0.50	0.75	1
DHN	0.70	0.75	0.70	1

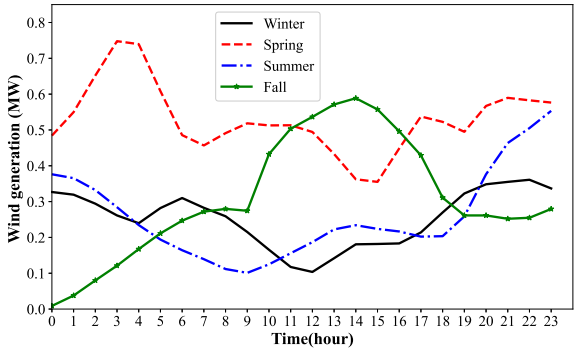

Figure 6: Wind generation profile (per MW)

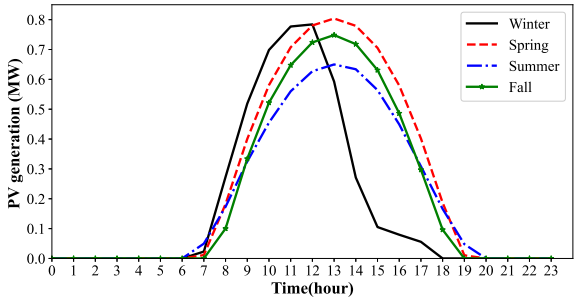

Figure 7: PV generation profile (per MW)

be located on the east coast of Florida, in the latitude range 27.95 to 28.00 and the longitude range -82.37 to -82.53. The related parameters for all candidate components and PDN's poles and conductors are listed in Tables. 3-6. Investment cost of PDN's lines includes isolation switch for each line. It is assumed that the poles supporting the distribution lines are southern pine wood poles since they are the dominant used in the understudied area. It is assumed that classes 2, 3, and 4 southern pine poles with 60, 30, and new ages exist in the PDN at the beginning of the study. In the planning period, the frequency of hurricane occurrence in each year is determined using a Poisson probability distribution function according to the climatic information of the understudied area. The fragility curve of the poles is age-dependent. So, in each year of the study, the probability of pole failure

Table 3
Parameters of candidate components

Component	IC (10^6\$/MW)	Fixed OC (10^3\$/MW.year)	Lifetime (year)
CHP	0.95	19.8	25
WT	1.2	25	20
PV	1.5	18	25
P2G	1.15	50	20
BESS	1.58	15	15
TBS	0.40	12	20
GS	0.35	8	20
EB	0.20	4	20
GB	0.18	12	30
TS	0.12	10	35

Table 4
Parameters of distribution lines

Component	IC (10^6\$/km)	Fixed OC (10^3\$/km.year)	Lifetime (year)
Power line	0.15	1	40
Pipeline	0.16	1.5	40

Table 5
Parameters of PDN's poles

Class	Installation (\$/pole)	Purchase (\$/pole)	Height (m)	Diameter (m)
2	Normal:2500 Emergency:4000	708	13.7	Top:0.20 Ground:0.33
3		544	13.7	Top:0.19 Ground:0.30
4		479	13.7	Top:0.17 Ground:0.28

Table 6
Parameters of PDN's conductor and accessories

Component	Cost (\$/km)	Impedance (Ω/km)	Max current (Amp)
Conductor (ACSR otter)	770	0.343+j0.328	270
Other	3850	-	-

is determined using updated fragility curves. Therefore, it is possible that in year one, a specific pole in the PDN is resilient, while in the tenth year of the planning, in the same scenario, the pole will be introduced as a high-risk pole in the face of the hurricane. Wind profile scenarios shown in Fig. 8 are extracted using Holland's model in (71) for categories 1, 2, and 3 of the Saffir-Simpson hurricane scale classification.

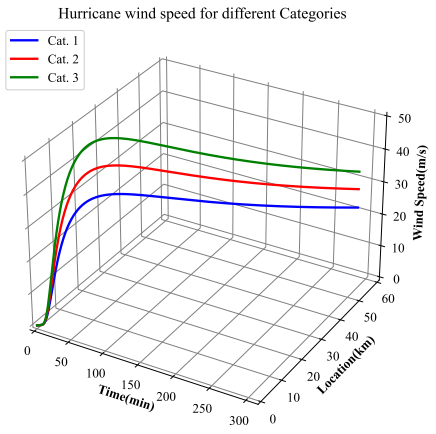

Figure 8: Hurricane's wind speed profiles

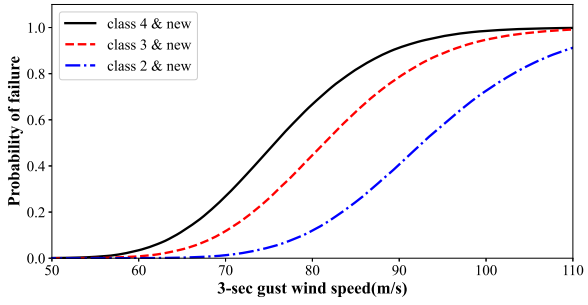

Figure 9: PDN's poles with different classes fragility curves

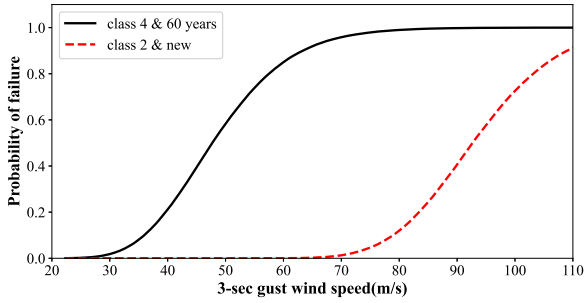

Figure 10: The worst and best fragility curve cases

As can be seen, hurricane's Wind profiles are displayed in a three-dimension curve according to the location and time. Fig. 9 and 10 are presented to determine the effect of age and class of poles on fragility curves. Fig. 9 shows the fragility curves of new poles with different ages, while Fig. 10 expresses the best and worst cases of fragility in the system. Table. 7 shows the priority of candidate lines for reinforcement and the priority of candidate tie-line for installation in the planning period in the PDN for case 1. The priorities, as mentioned earlier, are obtained using (73) and (74), respectively. Priority lists in each year of the planning are obtained in stage 2 and sent to stage 1. The reinforced lines and installed tie-lines are determined by solving the stage 1 optimization problem. As shown in Table. 7, power line 23 in the PDN is reinforced in year 1, but by increasing the pole ages and considering the high wind intensity on this line in the hurricane track, it encounters an outage in the tenth year of the planning. Nevertheless, considering the criteria that each PDN's lines can be reinforced only once in the planning period, this line is not in the list of reinforced lines in the tenth year of the planning in case 3. Table. 8 shows the economic results of the three case studies. The net present values (NPV) of investment cost (IC), operation cost (OC), energy purchasing from the upstream grid cost (EPC), and resilience improvement cost (RC) are listed in this table. In Table. 8 the row related to the IDN in the network column depicts the summation of costs in the PDN, GDN, and DHN. According to the results of studies, the total cost of stage 1 optimization objective function in the fourth scenario is lower than in other scenarios. The main reason is reducing costs due to power outages and damage to the networks by adding resilience improvement planning to the integrated expansion planning problem. The imposed cost of the distribution network's energy outages and failure is called resilience cost in this paper. The resilience cost in case 3 is just 9.24% of case 1, proving the significance and necessity of planning for resilience improvement. Also, the resilience cost of case 1 and case 3 comprise 9.24% and 0.35% of the total cost, respectively. It is worth noting that in this paper, just hurricane is considered; if other HR events or a combination of events be considered, the resilience cost would be a more significant share of the total cost. In case 2, the reconfiguration is added as a solution for improving resilience, but the resilience cost, in this case, is still more than twice that of case 3 which PDN lines reinforcement is added as a resilience improvement alternative in the planning. In order to scrutiny the technical details of the proposed IDNSEP case studies, some noteworthy results are presented in the continuation of this section. Fig. 11 shows the IDNs resilience curve using the proposed RI in (69) for the first, fifth, and tenth years of the planning. In this way, resilience improvement of IDNs during the 10-year IDNSEP can be evaluated. As shown in Fig. 11, the RI of the IDNs has the best values in case 3 and the worst in case 1. The resilience curve of case 3 has a better condition than case 2, which expresses that line reinforcement as a resilience improvement tool is more effective than tie-lines installation and network reconfiguration. The resilience curve of year 5 has a worse condition in cases 1 and 2 but is better in case 3. First, because of CHP units installation, the interdependency of the PDN and the DHN increases and impacts the resilience of the DHN by the outages in the PDN. Second, as the pole age increases, the probability of its outage increases, and without a reinforcement plan, the power outages may increase in the hurricane events. In the fifth year of case 3, the RI has its maximum possible value because, with the

Table 7
Stage 2 output results in the planning period

Year	Reinforcement list (Line No.)	Priority	Reinforced (Line No.)	Candidate tie-line (Tie-line No.)	Priority	Installed (Tie-line No.)
1	5,6,7,8,9,10,11,25 26,27,28,29,30,23,24	1,2,3,4,5,6,15,7 8,9,11,10,12,13,14	5,6,7,8,9,10,25,26	37,38,39,40,41	2,5,1,4,3	39,37,41
2	11,27,28,29,30,23,24	7,1,3,2,4,5,6	11,27,28,29,30,23,24	38,40	2,1	-
10	23	1	-	-	-	-

Table 8
Economic results of case studies

Case	Network	Net present value (10^6\$)				
		IC	OC	EPC	RC	Total
1	PDN	8.618	3.798	4.186	0.924	17.526
	GDN	1.874	3.395	4.113	0.134	9.516
	DHN	0.662	2.040	2.369	0.111	5.182
	IDN	11.154	9.233	10.668	1.169	32.224
2	PDN	7.892	4.017	4.620	0.553	17.082
	GDN	1.874	3.419	4.226	0.116	9.635
	DHN	0.645	2.073	2.195	0.095	5.008
	IDN	10.411	9.509	11.041	0.764	31.707
3	PDN	8.228	3.732	4.538	0.048	16.546
	GDN	1.717	3.274	4.124	0.044	9.159
	DHN	0.688	2.125	2.250	0.016	5.079
	IDN	10.633	9.131	10.912	0.108	30.784

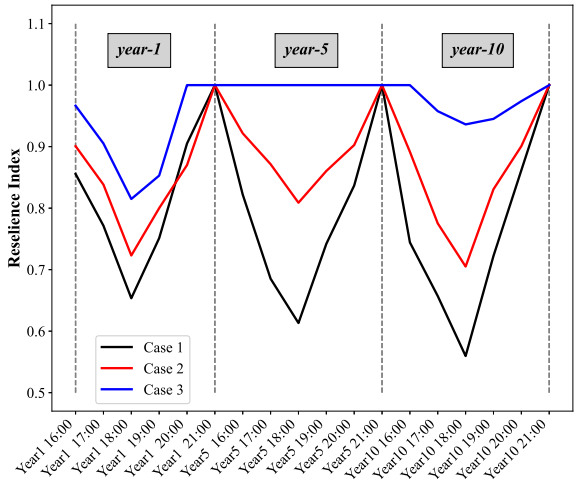

Figure 11: Resilience curves of the IDNs in case studies

implementation of reinforcement plan, all the poles with the probability of failure more than the threshold probability value are reinforced, and therefore no outage occurred in the PDN. The resilience curve of cases 1 and 2 in the tenth

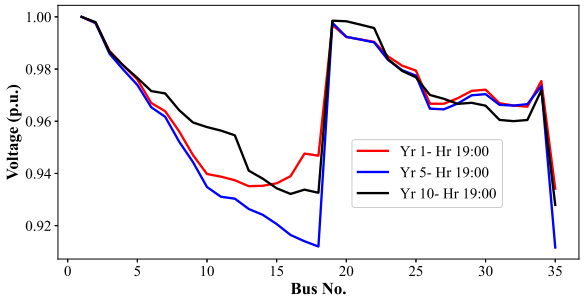

Figure 12: Voltage profile in normal condition of case 1

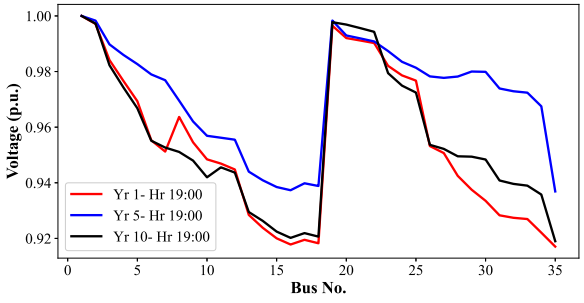

Figure 13: Voltage profile in normal condition of case 3

year has gotten worse for the same reasons mentioned above. The resilience curve of case 3 is worsened in the tenth year rather than the fifth year of the planning because the failure probability of power line 10 is more than the threshold value and needs to be reinforced. However, it is failed due to the considered constraint; each line can be reinforced only once in the planning period. For the operation phase of IDNs, voltage, pressure, and temperature in the PDN, GDN, and DHN in the worst normal and emergency conditions have been investigated.The voltage profile of PDN's normal condition for cases 1 and 3 are given in Fig. 12 and 13. These figures reveal the voltage profiles of PDN buses for years 1, 5, and 10 of planning in the maximum demand hour, 19:00. Fig. 14 and Fig. 15 depict the voltage profiles in the PDN in the worst condition, hour 18:00, in cases 1 and 3, respectively. Power line 23 in the PDN is reinforced in year 1 of case 3 planning, but with increasing the pole

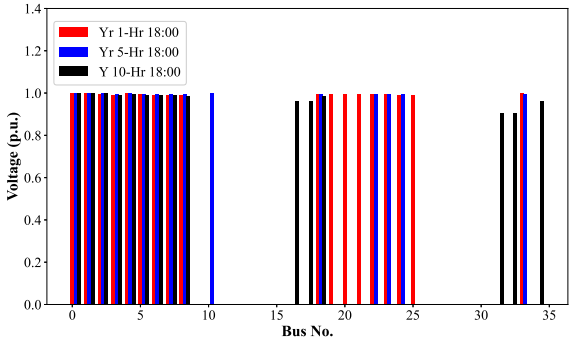

Figure 14: Voltage profile in emergency condition of case 1

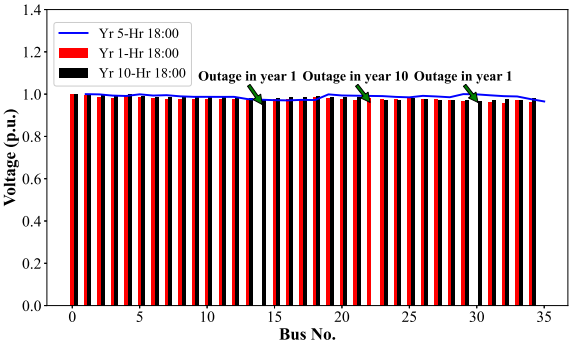

Figure 15: Voltage profile in emergency condition of case 3

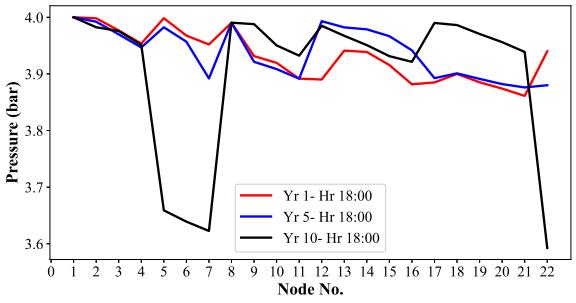

Figure 16: Pressure profile in emergency condition of case 3

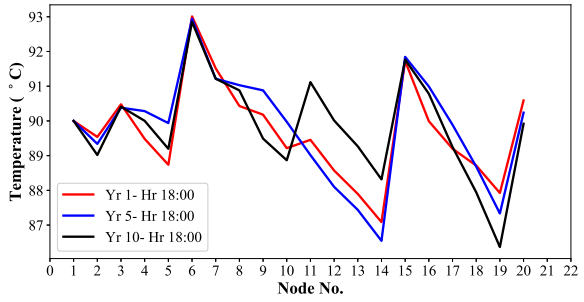

Figure 17: Temperature profile in emergency condition of case3

ages and considering the high wind intensity on this line in the hurricane track, it encounters outage in the tenth year of the planning. As given in Fig. 14, the voltage profile in the emergency condition of case 1 experiences the worst profile in the tenth year with 20 lines outage while Fig. 15 shows a noticeable line outage reduction in case 3, which in the worst condition experiences 2 line outages in the first year of planning. Fig. 16 and Fig. 17 show nodes gas pressure in the GDN, and nodes temperature in the DHN for emergency conditions in case 3. According to the results of the studies, in all cases, operation variables are within the permissible range. Gas pressure in the GDN is coupled to the PDN using power lines which connect bus 24 and bus 27 of the PDN to compressors placed between nodes 5-9 and nodes 17-18 in the GDN, respectively. In the emergency condition of the first year in case 3, bus 27 encounters an outage due to the outage of line 26 in the PDN; consequently, the related compressor in the GDN is forced to act as a regular pipeline. Therefore, as shown in Fig. 16, the gas pressure drops and leads to load shedding in nodes 18, 19, 20, and 21 in the GDN. Similarly, in the emergency condition of the tenth year in case 3, due to outage of line 23 in the PDN, the related compressor acts as a regular pipeline, consequently causes a pressure drop and load shed in nodes 5, 6,7, and 22 in the GDN. In the tenth year of planning, the dependence between the DHN and the PDN is maximized by installing CHP units, so by the outage of CHP connected bus in the PDN, buses 11 and 29 in case 1, supplied heat in the DHN is reduced, which leads to a decrease in the temperature of the nodes. Consequently, part of the demand is not supplied in the DHN and decreases the RI of the IDNs. In case 3, with the PDN line reinforcement strategy in the planning, line outage is largely prevented; as a result, the temperature profile in the tenth year of case 3 shown in Fig. 17 has a significant improvement, and there is no load shedding in this case. For better comparison, the lowest temperature of the nodes in the DHN is $83.1°C$ in case 1 and $86.4°C$ in case 3. Adjusting the parameters in the LADMMPSAP significantly affects the convergence of the solution and its speed. Determining the exact coefficients of the parameters is problem-based, so multiple choices are tried. The fixed and adaptive updating mechanisms for penalty parameters have been studied, based on which a dynamic μ makes the convergence faster. Also, the parameters of μ^0 and ρ_0 can be tuned easily when the adaptive penalty is used. For fast convergence, parameters are suggested, as given in Appendix. B. The parameter ρ should be chosen such that $\mu^{(k)}$ increases steadily onward with iterations. To obtain the ground truth solution OF^* for measuring the relative errors in the solutions, LADMMPSAP with 2000 iterations with $\mu_{max} = 1000$, $\rho_0 = 1$ with a conservative approach runs. This number of iterations is far more than necessary. The obtained results are considered as the optimum results. Then, using (80), the relative error in the solutions of each iteration

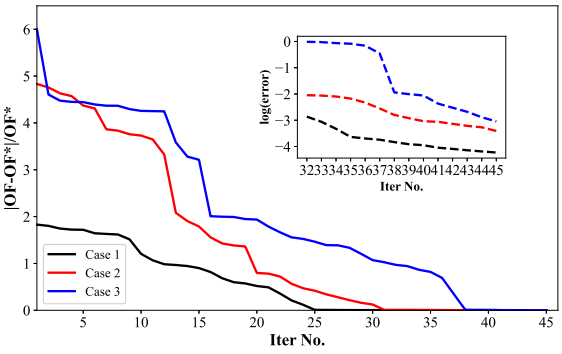

Figure 18: Convergence curve of case studies

is obtained, and the convergence curve is shown in Fig. 18.

$$OF^{error} = \frac{|OF - OF^*|}{OF^*} \tag{80}$$

As expected, the problem converges later in case 3 because a more complicated problem is solved due to considering reconfiguration as well as reinforcement strategy in the optimization. Dash line curves show the relative error's logarithm in iterations 28 to 41. It shows that cases 1, 2, and 3 converge in iteration 33, 40, and 45, respectively. The convergence is completed when the imbalance amount in (84) has reached the boundary condition 0.001.

5. Conclusion

This paper proposed a two-stage resilience-constrained expansion planning for integrated power, gas, and heat distribution networks. The optimal size and location of candidate generation and storage units were determined in stage 1. In stage 2, a resilience maximization problem was defined using the proposed RI and RII, which determine the priorities of PDN's reinforcement and tie-line installation to improve the IDNs resilience. The proposed centralized IDNSEP was a complex problem that was difficult to solve and time-consuming. Therefore, a new framework for integrating IDNs was proposed leveraging a coordinator unit responsible for coupling coordination among IDN's. Using the proposed LADMMPSAP, centralized IDNSEP was converted to decentralized sub-problems causing solving problems simpler and increasing the convergence speed. It was shown that the coordinator unit plays a vital role in accelerating problem solving, convergence and at the same time maintaining the independence of operation in the IDNs.The proposed resilience constrained IDNSEP with a limited budget was studied in a real scale IDNs with three case studies. The paper concluded that considering resilience in the long-term planning of the IDNs can simultaneously reduce the imposed cost to the system and improve the resilience of IDNs against HR events. Another implication of the results of this paper was that although reconfiguration is effective in improving the resilience of the IDNs and reducing costs, the impact of considering resilience in long-term planning is far more significant. It is recommended for future works to study the impacts of considering microgrids with private owners in expansion planning of IDNs and investigate the coordinator roles to couples IDNs to microgrids.

Algorithm I: The LADMMPSAP method

1.Calculation of $C_{N,t}^{sep(\kappa)}$ for separated sub-problems in each iteration k
2.Set initial value for x_r vector elements and constants $\varepsilon_1, \varepsilon_2, \varepsilon_3 > 0,\ \rho_0 > 1,\ \mu_{max} \gg 1 \gg \mu_0 > 0$
3.Solving the decentralized IDNSEP (75)-(77) with operation constraints and data exchange with coordinator
4.Parallel updating of x_r vector elements as following:
(r and r' presents two integrated elements in x_r)
$x_r^{(\kappa+1)} = \delta^{(\kappa)}(x_r - x_{r'}^{(\kappa)}) + \frac{\lambda^{(\kappa)}}{2}\|(x_r - x_{r'}^{(\kappa)}) + (\frac{x_r^{(\kappa)} - x_{r'}^{(\kappa)}}{\lambda^{(\kappa)}})\|^2$
5.Updating $\lambda^{(\kappa)}$ and $\delta^{(\kappa)}$as following
$\delta^{(\kappa+1)} = \delta^{(\kappa)} + \mu^{(\kappa)}(x_r^{(\kappa+1)} - x_{r'}^{(\kappa+1)})$
$\lambda^{(\kappa)} = \sigma_r \mu^{(\kappa)}$
$\mu^{(\kappa+1)} = \min(\mu_{max}, \rho\mu^{(\kappa)})$
$\rho = \begin{cases} \rho_0 & \text{if } \mu^{(\kappa)} max(\sqrt{\sigma_r}\|x_r^{(\kappa+1)} - x_r^{(\kappa)}\|, r = 1, ..., 8) < \varepsilon_2 \\ 1 & \text{otherwise} \end{cases}$
6.Coordinator checks the below stop criteria, if they are not satisfied go to 2, otherwise stop
Error 1: $\|x_r^{(\kappa+1)} - x_{r'}^{(\kappa+1)}\|_2^2 < \varepsilon_1$
Error 2: $max(\sqrt{\sigma_r}\|x_r^{(\kappa+1)} - x_r^{(\kappa)}\|) < \varepsilon_2 \ \ \forall r = 1, ..., 8$
Error 3: $max(\|C_{N,t}^{sep(\kappa+1)} - C_{N,t}^{sep(\kappa)}\|) < \varepsilon_3 \ \ \forall N \in \Omega_N$

Appendix A LADMMPSAP Algorithm

In order to simplify the formulation in the algorithm, a general vector variable x_r as (A.1) is used to represent the variables exchanges between sub-problems.

$$x_r = \left\{ \begin{array}{l} q_{E,\hat{j}i,t}, q_{G,\hat{j}i,t}, P_{E,i\hat{k},t}, P_{H,i\hat{k},t}, \\ q_{G,j\hat{k},t}, q_{H,j\hat{k},t}, P_{E,\hat{i}j,t}, P_{G,\hat{i}j,t} \end{array} \right\} \tag{A.1}$$

Appendix B Data and simulation parameters

Technical data of lines and pipelines, simulation parameters, and geographical coordination of PDN's buses are given in Tables. B.4-B.3.

Table B.1
PDN buses geographical coordination

Bus No.	Coordinate (Longitude,Latitude)	Bus No.	Coordinate (Longitude,Latitude)	Bus No.	Coordinate (Longitude,Latitude)
1	(82.7500W, 28.0650N)	12	(82.6240W, 28.0650N)	23	(82.7270W, 28.0750N)
2	(82.7400W, 28.0650N)	13	(82.6140W, 28.0650N)	24	(82.7270W, 28.0850N)
3	(82.7270W, 28.0650N)	14	(82.6060W, 28.0650N)	25	(82.7180W, 28.0850N)
4	(82.7150W, 28.0650N)	15	(82.5930W, 28.0650N)	26	(82.6900W, 28.0730N)
5	(82.7000W, 28.0650N)	16	(82.5830W, 28.0650N)	27	(82.6790W, 28.0730N)
6	(82.6900W, 28.0650N)	17	(82.5830W, 28.0740N)	28	(82.6690W, 28.0820N)
7	(82.6780W, 28.0650N)	18	(82.5830W, 28.0850N)	29	(82.6570W, 28.0820N)
8	(82.6650W, 28.0650N)	19	(82.7350W, 28.0550N)	30	(82.6560W, 28.0820N)
9	(82.6570W, 28.0650N)	20	(82.7250W, 28.0480N)	31	(82.6480W, 28.0820N)
10	(82.6440W, 28.0650N)	21	(82.7150W, 28.0480N)	32	(82.6390W, 28.0820N)
11	(82.6350W, 28.0650N)	22	(82.7040W, 28.0480N)	33	(82.6280W, 28.0820N)
34	(82.7080W, 28.0850N)	35	(82.5710W, 28.0650N)	-	-

Table B.2
Data of lines and pipelines

Network	Existing lines\pipelines									Candidate lines\pipelines		
	Line No.	Line (i-j)	Length (km)	Line No.	Line (i-j)	Length (km)	Line No.	Line (i-j)	Length (km)	Line No.	Line (i-j)	Length (km)
PDN	1	1-2	1	12	12-13	1	23	23-24	1	33	25-34	1
	2	2-3	1.3	13	13-14	0.8	24	24-25	0.9	34	6-34	1.3
	3	3-4	1.2	14	14-15	1.3	25	6-26	0.9	35	16-35	1.2
	4	4-5	1.5	15	15-16	1	26	26-27	1.1	36	18-35	2
	5	5-6	1	16	16-17	0.9	27	27-28	1.2		**Tie-lines**	
	6	6-7	1.2	17	17-18	1.4	28	28-29	1	37	25-29	2.5
	7	7-8	1.3	18	2-19	1.3	29	29-30	0.8	38	8-21	1.7
	8	8-9	0.8	19	19-20	1.2	30	30-31	0.9	39	12-22	3.1
	9	9-10	1.3	20	20-21	1	31	31-32	1.1	40	9-15	2
	10	10-11	0.9	21	21-22	1.1	32	32-33	0.8	41	18-33	1.2
	11	11-12	1.1	22	3-23	1	-	-	-	-	-	-
GDN	1	1-2	1	8	8-9	1.1	15	15-16	1	20	7-22	0.8
	2	2-3	1	9	9-10	0.9	16	11-17	1.2	21	12-22	1.4
	3	3-4	0.8	10	10-11	0.8	17	17-18	1.5	22	20-21	1.1
	4	4-5	1.3	11	11-12	0.9	18	18-19	0.9	23	16-21	1.1
	5	5-6	0.9	12	12-13	0.7	19	19-20	1	-	-	-
	6	6-7	1.1	13	13-14	1	-	-	-	-	-	-
	7	5-9	1.4	14	14-15	1	-	-	-	-	-	-
DHN	1	1-2	0.6	7	7-8	1.2	13	13-14	0.5	18	14-20	1.1
	2	2-3	0.7	8	8-9	1	14	5-15	1.2	19	6-20	1.1
	3	3-4	0.7	9	9-10	1	15	15-16	1.1	20	18-19	1
	4	4-5	1	10	3-11	0.9	16	16-17	0.9	21	8-19	1
	5	5-6	1.1	11	11-12	0.6	17	17-18	1.1	-	-	-
	6	6-7	0.9	12	12-13	0.7	-	-	-	-	-	-

Table B.3
Data of interconnected lines and pipelines

Existing lines\pipelines				Candidate lines\pipelines			
Type	Network (From-To)	Bus\Node No.	Length (km)	Type	Network (From-To)	Bus\Node No.	Length (km)
Pipeline	G-H	17-15	0.6	Pipeline	G-H	3-6	0.6
Pipeline	E-H	5-3	0.3	Pipeline	G-E	7-29	0.5
Line	E-G	24-$Co_{5,9}$	0.4	Pipeline	G-E	8-23	0.3
Line	E-G	27-$Co_{17,18}$	0.5	Pipeline	G-E	9-5	0.5
Line	E-H	21-$Pu_{5,15}$	0.5	Pipeline	G-E	20-11	0.4
-	-	-	-	Pipeline	E-G	14-16	0.5
-	-	-	-	Pipeline	E-G	31-13	0.8
-	-	-	-	Pipeline	E-H	23-13	0.4
-	-	-	-	Pipeline	E-H	29-8	0.7
-	-	-	-	Pipeline	E-H	11-17	0.4
-	-	-	-	Line	E-H	9-11	0.7

Table B.4
Simulation parameters

Parameter	Value	Parameter	Value
$\overline{S}_{E,t}^{Imp}$	10 MVA	$\eta_{E,s}^{ch}, \eta_{E,s}^{dis}$	0.95
$\xi_{5,9}, \xi_{17,18}$	1.08,1.12	$\eta_{G,s}^{ch}, \eta_{G,s}^{dis}$	0.95
$\underline{CR}, \overline{CR}$	1.2	$\eta_{H,s}^{ch}, \eta_{H,s}^{dis}$	0.92
k_1	25 Wh/m^3	$\eta_{i,g}^{P2G}, \eta_{i,g}^{EB}, \eta_{i,g}^{GB}$	0.65,0.98,0.90
k_2	1.3	$\eta_{i,g}^{CHP,e}, \eta_{i,g}^{CHP,hl}$	2.4,0.03
$\underline{V}_i, \overline{V}_i$	0.9,1.1 p.u.	$\beta_{i,g}^{CHP}$	1.2
P_{Th}^{f}	0.1	μ^0, ρ_0	0.01,2
$\varepsilon_1, \varepsilon_2, \varepsilon_3$	0.001	μ_{max}	100

References

[1] H. Fan, Q. Yuan, S. Xia, J. Lu, Z. Li, Optimally coordinated expansion planning of coupled electricity, heat and natural gas infrastructure for multi-energy system, IEEE Access 8 (2020) 91139–91149.

[2] X. Wang, M. Shahidehpour, C. Jiang, Z. Li, Resilience enhancement strategies for power distribution network coupled with urban transportation system, IEEE Transactions on Smart Grid 10 (2019) 4068–4079.

[3] B. P. Koirala, E. Koliou, J. Friege, R. A. Hakvoort, P. M. Herder, Energetic communities for community energy: A review of key issues and trends shaping integrated community energy systems, Renewable and Sustainable Energy Reviews 56 (2016) 722–744.

[4] M. Farrokhifar, Y. Nie, D. Pozo, Energy systems planning: A survey on models for integrated power and natural gas networks coordination, Applied Energy 262 (2020) 114567.

[5] V. Khaligh, M. O. Buygi, A. A. Moghaddam, J. M. Guerrero, Integrated expansion planning of gas-electricity system: A case study in iran, in: 2018 International Conference on Smart Energy Systems and Technologies (SEST), 2018, pp. 1–6. doi:10.1109/SEST.2018.8495704.

[6] R.-B. R. V. A. OJEDA-ESTEYBAR, D.M., Integrated operational planning of hydrothermal power and natural gas systems with large scale storages, J. Mod. Power Syst. Clean Energy 5 (2017) 299–313.

[7] C. He, L. Wu, T. Liu, Z. Bie, Robust co-optimization planning of interdependent electricity and natural gas systems with a joint n-1 and probabilistic reliability criterion, IEEE Transactions on Power Systems 33 (2018) 2140–2154.

[8] X. Zhang, L. Che, M. Shahidehpour, A. S. Alabdulwahab, A. Abusorrah, Reliability-based optimal planning of electricity and natural gas interconnections for multiple energy hubs, IEEE Transactions on Smart Grid 8 (2017) 1658–1667.

[9] V. Khaligh, A. Anvari-Moghaddam, Stochastic expansion planning of gas and electricity networks: A decentralized-based approach, Energy 186 (2019) 115889.

[10] T. Ding, Y. Hu, Z. Bie, Multi-stage stochastic programming with nonanticipativity constraints for expansion of combined power and natural gas systems, IEEE Transactions on Power Systems 33 (2018) 317–328.

[11] B. Odetayo, M. Kazemi, J. MacCormack, W. D. Rosehart, H. Zareipour, A. R. Seifi, A chance constrained programming approach to the integrated planning of electric power generation, natural gas network and storage, IEEE Transactions on Power Systems 33 (2018) 6883–6893.

[12] Q. Zeng, B. Zhang, J. Fang, Z. Chen, A bi-level programming for multistage co-expansion planning of the integrated gas and electricity system, Applied Energy 200 (2017) 192–203.

[13] X. Zhang, C. Bauer, C. L. Mutel, K. Volkart, Life cycle assessment of power-to-gas: Approaches, system variations and their environmental implications, Applied Energy 190 (2017) 326–338.

[14] J. Liang, W. Tang, Stochastic multistage co-planning of integrated energy systems considering power-to-gas and the cap-and-trade market, International Journal of Electrical Power & Energy Systems 119 (2020) 105817.

[15] M. A. Mirzaei, M. Nazari-Heris, B. Mohammadi-Ivatloo, K. Zare, M. Marzband, A. Anvari-Moghaddam, A novel hybrid framework for co-optimization of power and natural gas networks integrated with emerging technologies, IEEE Systems Journal 14 (2020) 3598–3608.

[16] N. Linna, L. Weijia, W. Fushuan, X. Yusheng, Z. Zhaoyang, DONGa nd Yu, Z. Rui, Optimal operation of electricity, natural gas and heat systems considering integrated demand responses and diversified storage devicess, J. Mod. Power Syst. Clean Energy 6 (2018) 423–437.

[17] Y. Lei, D. Wang, H. Jia, J. Chen, J. Li, Y. Song, J. Li, Multi-objective stochastic expansion planning based on multi-dimensional correlation scenario generation method for regional integrated energy system integrated renewable energy, Applied Energy 276 (2020) 115395.

[18] X. Liu, P. Mancarella, Modelling, assessment and sankey diagrams of integrated electricity-heat-gas networks in multi-vector district energy systems, Applied Energy 167 (2016) 336–352.

[19] J. Wang, Z. Hu, S. Xie, Expansion planning model of multi-energy system with the integration of active distribution network, Applied Energy 253 (2019) 113517.

[20] X. Zhang, M. Shahidehpour, A. Alabdulwahab, A. Abusorrah, Optimal expansion planning of energy hub with multiple energy infrastructures, IEEE Transactions on Smart Grid 6 (2015) 2302–2311.

[21] W. Huang, N. Zhang, J. Yang, Y. Wang, C. Kang, Optimal configuration planning of multi-energy systems considering distributed renewable energy, IEEE Transactions on Smart Grid 10 (2019) 1452–1464.

[22] M. H. Amirioun, F. Aminifar, M. Shahidehpour, Resilience-promoting proactive scheduling against hurricanes in multiple energy carrier microgrids, IEEE Transactions on Power Systems 34 (2019) 2160–2168.

[23] J. Najafi, A. Peiravi, A. Anvari-Moghaddam, J. M. Guerrero, Resilience improvement planning of power-water distribution systems with multiple microgrids against hurricanes using clean strategies, Journal of Cleaner Production 223 (2019) 109–126.

[24] J. Najafi, A. Peiravi, A. Anvari-Moghaddam, J. Guerrero, An efficient interactive framework for improving resilience of power-water distribution systems with multiple privately-owned microgrids, International Journal of Electrical Power & Energy Systems 116 (2020) 105550.

[25] W. M. Patricola, C.M., Anthropogenic influences on major tropical cyclone events, Nature 563 (2018) 339–346.

[26] G. Muñoz-Delgado, J. Contreras, J. M. Arroyo, Distribution network expansion planning with an explicit formulation for reliability assessment, IEEE Transactions on Power Systems 33 (2018) 2583–2596.

[27] C. Lv, H. Yu, P. Li, K. Zhao, H. Li, S. Li, Coordinated operation and planning of integrated electricity and gas community energy system with enhanced operational resilience, IEEE Access 8 (2020) 59257–59277.

[28] C. Shao, M. Shahidehpour, X. Wang, X. Wang, B. Wang, Integrated planning of electricity and natural gas transportation systems for enhancing the power grid resilience, IEEE Transactions on Power Systems 32 (2017) 4418–4429.

[29] Y. Wen, X. Qu, W. Li, X. Liu, X. Ye, Synergistic operation of electricity and natural gas networks via admm, IEEE Transactions on Smart Grid 9 (2018) 4555–4565.

[30] C. He, L. Wu, T. Liu, M. Shahidehpour, Robust co-optimization scheduling of electricity and natural gas systems via admm, IEEE Transactions on Sustainable Energy 8 (2017) 658–670.

[31] C. Chen, B. He, Y. Ye, X. Yuan, The direct extension of admm for multi-block convex minimization problems is not necessarily convergent, Mathematical Programming 155 (2016) 57–79.

[32] Z. Lin, H. Zhang, Chapter 4 - optimization algorithms, in: Z. Lin, H. Zhang (Eds.), Low-Rank Models in Visual Analysis, Computer Vision and Pattern Recognition, Academic Press, 2017, pp. 55–110. URL: https://www.sciencedirect.com/science/article/pii/B9780128127315000044. doi:https://doi.org/10.1016/B978-0-12-812731-5.00004-4.

[33] A. Gholami, T. Shekari, F. Aminifar, M. Shahidehpour, Microgrid scheduling with uncertainty: The quest for resilience, IEEE Transactions on Smart Grid 7 (2016) 2849–2858.

[34] P. Liu, T. Ding, Z. Zou, Y. Yang, Integrated demand response for a load serving entity in multi-energy market considering network constraints, Applied Energy 250 (2019) 512–529.

[35] Z. Li, W. Wu, M. Shahidehpour, J. Wang, B. Zhang, Combined heat and power dispatch considering pipeline energy storage of district heating network, IEEE Transactions on Sustainable Energy 7 (2016) 12–22.

[36] J. Li, J. Fang, Q. Zeng, Z. Chen, Optimal operation of the integrated electrical and heating systems to accommodate the intermittent renewable sources, Applied Energy 167 (2016) 244–254.

[37] Q. Zeng, B. Zhang, J. Fang, Z. Chen, A bi-level programming for multistage co-expansion planning of the integrated gas and electricity system, Applied Energy 200 (2017) 192–203.

[38] A. Arif, S. Ma, Z. Wang, J. Wang, S. M. Ryan, C. Chen, Optimizing service restoration in distribution systems with uncertain repair time and demand, IEEE Transactions on Power Systems 33 (2018) 6828–6838.

[39] S. Ma, L. Su, Z. Wang, F. Qiu, G. Guo, Resilience enhancement of distribution grids against extreme weather events, IEEE Transactions on Power Systems 33 (2018) 4842–4853.

[40] G. J. Holland, J. I. Belanger, A. Fritz, A revised model for radial profiles of hurricane winds, Monthly Weather Review 138 (2010) 4393–4401.

[41] G. Li, P. Zhang, P. B. Luh, W. Li, Z. Bie, C. Serna, Z. Zhao, Risk analysis for distribution systems in the northeast u.s. under wind storms, IEEE Transactions on Power Systems 29 (2014) 889–898.

[42] M. Ouyang, L. Dueñas-Osorio, Multi-dimensional hurricane resilience assessment of electric power systems, Structural Safety 48 (2014) 15–24.

[43] M. Baran, F. Wu, Network reconfiguration in distribution systems for loss reduction and load balancing, IEEE Transactions on Power Delivery 4 (1989) 1401–1407.

[44] T. Jiang, H. Deng, L. Bai, R. Zhang, X. Li, H. Chen, Optimal energy flow and nodal energy pricing in carbon emission-embedded integrated energy systems, CSEE Journal of Power and Energy Systems 4 (2018) 179–187.

[45] Weather aned energy dataset, 2019. URL: https://www.renewables.ninja/, (accessed 27 June 2021).

[46] N. Growe-Kuska, H. Heitsch, W. Romisch, Scenario reduction and scenario tree construction for power management problems, in: 2003 IEEE Bologna Power Tech Conference Proceedings, volume 3, 2003, pp. 7 pp. Vol.3–. doi:10.1109/PTC.2003.1304379.